

Unsupervised Methods for Video Quality Improvement: A Survey of Restoration and Enhancement Techniques

Alexandra Malyugina^{1*}, Yini Li¹, Joanne Lin¹,
Nantheera Anantrasirichai¹

^{1*}Visual Information Laboratory, University of Bristol, Merchant
Venturers Building Woodland Road, Bristol, BS8 1UB, UK.

*Corresponding author(s). E-mail(s): alex.malyugina@bristol.ac.uk;
Contributing authors: ub24017@bristol.ac.uk; joanne.lin@bristol.ac.uk;
n.anantrasirichai@bristol.ac.uk;

Abstract

Video restoration and enhancement are critical not only for improving visual quality, but also as essential pre-processing steps to boost the performance of a wide range of downstream computer vision tasks. This survey presents a comprehensive review of video restoration and enhancement techniques with a particular focus on unsupervised approaches. We begin by outlining the most common video degradations and their underlying causes, followed by a review of early conventional and deep learning methods-based, highlighting their strengths and limitations. We then present an in-depth overview of unsupervised methods, categorise by their fundamental approaches, including domain translation, self-supervision signal design and blind spot or noise-based methods. We also provide a categorization of loss functions employed in unsupervised video restoration and enhancement, and discuss the role of paired synthetic datasets in enabling objective evaluation. Finally, we identify key challenges and outline promising directions for future research in this field.

Keywords: video restoration, video enhancement, unsupervised learning, synthetic data

Contents

1	Introduction	4
2	Basics of Video Restoration and Enhancement	5
2.1	Common Degradation Problems in Videos	6
2.1.1	Blur	6
2.1.2	Noise	6
2.1.3	Continuous Scattering Degradations	7
2.1.4	Transient Particulate Degradations	8
2.1.5	Complex Degradations	9
2.2	Traditional Video Enhancement and Restoration Methods	9
2.3	Supervised Deep Learning Based Video Restoration and Enhancement Techniques	13
2.3.1	Convolutional Neural Networks	13
2.3.2	Recurrent Neural Networks	13
2.3.3	Transformer-Based Networks	14
3	Unsupervised Learning in Video Restoration and Enhancement	15
3.1	Unsupervised, Self-Supervised, and Zero-Shot Learning for Video Tasks	15
3.2	Domain Translation with Unpaired Learning	16
3.3	Self-Supervised Signal Design	17
3.3.1	Blind-Spot and Noise-Based Methods	17
3.3.2	Optimization-Unrolling Methods	19
3.3.3	Deep Plug-and-Play	19
3.4	Consistency-Based Methods	20
3.4.1	Temporal consistency	20
3.4.2	Semantic consistency	21
3.5	Degradation-Aware Methods	21
3.5.1	Degradation Simulation and Re-Degradation	21
3.6	Prior-Based Methods	22
3.6.1	Physics-Based Priors	22
3.6.2	Learning-based Priors	23
4	Loss Functions for Unsupervised Video Restoration and Enhancement	24
4.1	Reference-Fidelity Losses	26
4.2	Data Consistency Losses	27
4.2.1	Spatial Data Consistency Losses	27
4.2.2	Temporal Data Consistency Losses	27
4.3	Prior-based Losses	28
4.4	Adversarial Losses	28
5	Synthetic Distorted Data Methods	29
5.1	Synthetic Blur	29
5.2	Synthetic Noise	30

5.3	Synthetic Low Light	31
5.4	Synthetic Light Attenuation	32
5.5	Synthetic Atmospheric Turbulence	32
6	Challenges and Open Problems	33
7	Conclusion	34

1 Introduction

Videos captured under real-world conditions often exhibit various degradations, including poor illumination, motion blur, out-of-focus, noise, compression artifacts, low contrast, flicker, and temporal inconsistencies. These not only degrade visual quality but also impair downstream tasks such as object tracking, recognition, segmentation, optical flow, and depth estimation, potentially resulting in false negatives, misclassifications, or system failures, as reported in [1–3]. Consequently, video quality enhancement has become a critical research focus, especially for footage acquired in uncontrolled or adverse environments.

Broadly, two related but distinct objectives are commonly addressed in this context: *restoration* and *enhancement*. Restoration focuses on recovering a clean video from its degraded counterpart by assuming a known or estimated corruption model, such as sensor noise, motion blur, compression artifacts, or missing data. In contrast, enhancement aims to improve the perceptual quality of video — adjusting attributes like dynamic range, contrast, color balance, or sharpness — without requiring explicit knowledge of the degradation process. Restoration methods typically prioritise fidelity to an undistorted signal, while enhancement techniques focus on improving visual clarity and aesthetic appeal, which are often guided by more subjective criteria [4, 5]. In practice, the boundary between these two categories is often obscure: enhancing contrast may incidentally reduce blur, and deblurring may improve perceptual sharpness. Consequently, many modern methods are designed to address both tasks simultaneously, particularly in scenarios where degradations are complex or poorly characterised.

Traditionally, both restoration and enhancement tasks have been tackled using handcrafted filters and domain-specific priors [6, 7]. More recently, learning-based approaches, particularly those employing deep neural networks, have achieved significant progress in a wide range of *image* restoration and enhancement tasks. Many such tools are now available in both open-source and commercial software [8]. In contrast, *video*-based AI restoration and enhancement methods remain relatively nascent, hindered by a higher number of unknown parameters, limited datasets, greater computational complexity, and elevated memory requirements. A common workaround involves applying image-based models frame-by-frame, but this often introduces temporal inconsistencies [9]. Furthermore, the majority of existing methods for both image and video quality enhancement rely on paired training data, with degraded and reference sequences aligned spatially and temporally. Acquiring such data is expensive and often impractical in real-world scenarios such as surveillance, low-light natural history recordings, and historical archives, where high-quality ground truth is unavailable or cannot be reliably reconstructed.

This has motivated growing interest in unsupervised approaches that learn from unpaired or unlabeled data by leveraging inherent structures in video, such as temporal consistency [10], spatial redundancy [11], motion coherence [12], and statistical priors [13]. Without relying on explicit ground truth, unsupervised methods are particularly well suited for domain-adaptive video quality enhancement, where degradations are complex, unknown, or data-specific.

While numerous surveys exist on *image* restoration and enhancement, dedicated reviews of *video*-specific approaches remain limited. Existing works on video restoration [14], low-light video enhancement [15], and underwater video enhancement [16] primarily focus on supervised frameworks and associated loss functions. Although [15] briefly mentions self-supervised learning, the discussion is confined to image-based methods. Critically, these surveys overlook the expanding literature on unsupervised and weakly supervised video restoration and enhancement. Our paper aims to fill that gap by providing a focused review of methods that operate without paired ground truth, which is an increasingly important paradigm for real-world applications where annotated video data is difficult, costly or impractical to obtain.

In this survey, we present a structured overview of unsupervised methods for video restoration and enhancement. To provide context, we first briefly review classical and supervised approaches. We then categorise unsupervised techniques according to their methodological strategies and source of supervision. Furthermore, we provide a categorization of loss functions employed in unsupervised video restoration and enhancement. Finally, we describe the synthetic datasets for objective evaluation of unsupervised methods and discuss current challenges and open research questions. Our aim in this paper is to offer a critical synthesis of the current literature and a comprehensive foundation for future developments in video restoration and enhancement under unpaired supervision.

2 Basics of Video Restoration and Enhancement

Video restoration and enhancement are inherently ill-posed inverse problems, often admitting multiple valid solutions due to information loss during capture. These tasks become particularly challenging when attempting to reconstruct the original content from severely degraded observations. A common formulation expresses degradation as

$$I_{\text{obv}} = HI_{\text{idl}} + n, \quad (1)$$

where I_{idl} denotes the ideal (clean) signal, I_{obv} is the observed video, H represents an unknown distortion function, and n is additive noise. Many existing methods simplify this by assuming a space-invariant point spread function for H and Gaussian zero-mean noise for n . However, such assumptions fail to generalise to real-world scenarios involving complex environmental degradation, e.g., low-light conditions, dynamic non-stationary media, light scattering and absorption, which lead to a mix of blur, noise, color distortion, halo artifacts, and contrast reduction.

Moreover, real-world video restoration is not only ill-posed but also blind, as the degradation model and parameters are typically unknown. The noise characteristics, blur kernels, and degradation severity are often uncertain, necessitating blind restoration techniques that jointly estimate both the clean content and the underlying corruption model. This results in highly non-convex optimization problems, further compounding the difficulty of accurate video enhancement in uncontrolled environments.



Fig. 1: A video sequence fragment from GoPro Dataset [22], showing regions affected by motion blur



Fig. 2: An example of out-of-focus blur

2.1 Common Degradation Problems in Videos

Real-world videos frequently exhibit a range of artifacts resulting from different types of degradation, necessitating enhancement or restoration. In this subsection, we discuss the most common degradation types encountered in practice: blur, noise, low contrast, and low-light conditions.

2.1.1 Blur

Videos captured with moving cameras or objects often exhibit *motion blur*, particularly under long exposure times or high-speed movement. In video, motion blur manifests as smearing along moving edges and typically varies across frames. It is often temporally uncorrelated between successive frames [17]. Common causes include handheld camera shake, which results in global blur, and fast-moving objects, leading to local blur. Unlike still-image blur, video blur benefits from temporal redundancy: adjacent frames are often blurred differently, allowing sharp details in one frame to compensate for losses in another. This property underpins many video deblurring strategies [18].

Defocus blur (or *out-of-focus blur*) arises when scene elements fall outside the camera’s depth of field, resulting in a loss of sharpness [19]. *Atmospheric blur*, induced by air turbulence resulting from temperature variations across regions, distorts light propagation, particularly over long distances, and is commonly encountered in outdoor surveillance [20] and remote sensing applications [21]. Example of motion blur and out-of-focus blur are shown in Fig. 1 and Fig. 2, respectively .

2.1.2 Noise

In digital images and videos, noise manifests as random variations in pixel intensity or color, leading to degradation of fine details. In video, electronic noise is particularly prevalent, primarily originating from the camera sensor and associated circuitry. Typical sources include photon shot noise, read noise, and dark current noise [23], along with quantization noise (from analog-to-digital conversion) and transmission noise (from lossy or noisy communication channels). Noise is often modeled using a Gaussian distribution, or a Poisson–Gaussian mixture to account for both photon and electronic

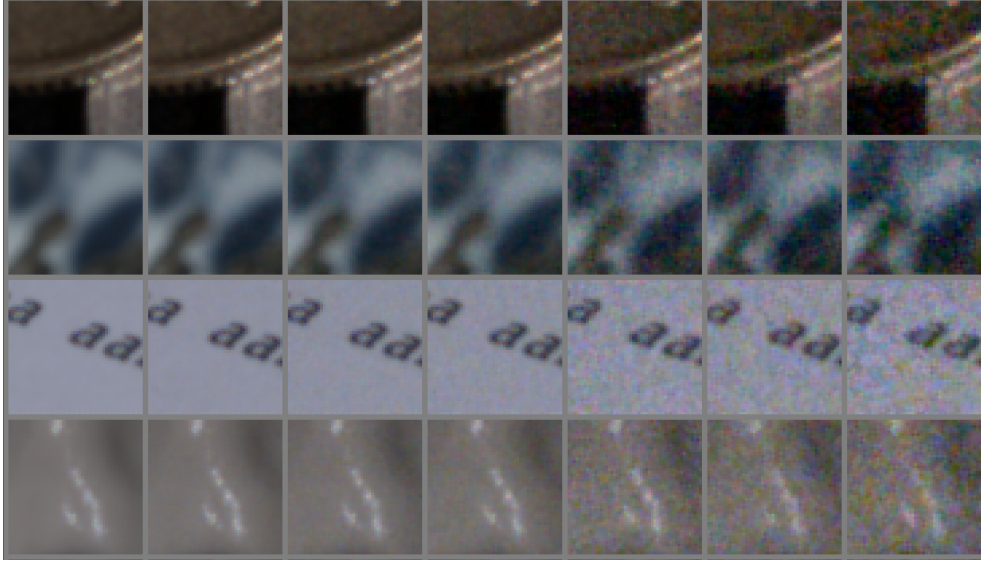


Fig. 3: Examples of sensor noise at different ISO levels (ISO = 1600, 6400, 12800, 64000, 102400, 160000); image patches from [25]

contributions [24]. Under well-lit conditions, noise tends to be minimal. However, in low-light environments, cameras increase sensor gain (e.g., through higher ISO settings), which amplifies both the signal and noise, often resulting in significantly noisier output. In video sequences, noise can appear as high-frequency grain, stemming from photon shot noise, as well as banding or artifacts introduced by readout and compression. Unlike motion blur, noise is typically temporally uncorrelated, assuming no in-camera temporal averaging or denoising. Examples of noisy patches are shown in Fig. 3, where the right images were captured under lower-light conditions. To maintain a consistent brightness level, higher ISO settings were applied, which introduced additional noise. Consequently, the darker scenes exhibit significantly higher noise due to the increased ISO sensitivity required in low-light environments.

2.1.3 Continuous Scattering Degradations

Outdoor videos captured in fog, mist, or polluted environments suffer from two primary phenomena [26]: *attenuation*, the loss of scene radiance due to absorption, and *airlight*, the additive scattered light from the atmosphere. Haze in digital images and videos is caused by suspended particles in the air, such as dust, smoke, and microscopic water droplets. These particles absorb and scatter light rays traveling from scene objects to the camera [27]. This process reduces contrast and alters color perception, particularly over long distances. In fluid environments, similar degradation is modeled by the Jaffe–McGlamery model [28, 29], which accounts for both absorption and scattering in participating media such as seawater. This model decomposes the captured image into three components: direct transmission, forward scattering,



Fig. 4: Low contrast and grey veil (haze) caused by atmospheric particles.



Fig. 5: Low contrast and blurry underwater footage

and backscattering. The scattering introduces a veiling luminance (or veiling light) that overlays the scene, obscuring textures and fine details. Consequently, hazy videos exhibit reduced visibility, loss of texture in distant regions, and desaturated colors. In underwater videos, these effects are further compounded by wavelength-dependent light attenuation, which causes severe color imbalance due to the differential absorption of red, green, and blue wavelengths, resulting in a strong bluish or greenish cast. The classic degradation model is shown as described in Eq. 2 [30]:

$$I(x) = J(x)t(x) + A[1 - t(x)], \quad (2)$$

where I is the observed image intensity, J the true scene radiance (i.e., the desired output), A the global atmospheric light (ambient veil color), which is typically assumed to be constant, and $t(x)$ the transmission map, representing the portion of scene radiance that reaches the camera after attenuation by atmospheric particles. The transmission map generally decreases with increasing scene depth. Dehazing involves estimating both A and $t(x)$ in order to recover the clean image $J(x)$. In video, haze can vary over time due to changes in weather conditions, illumination intensity and direction, or camera motion (e.g., moving into or out of a foggy region). Video degradation, caused by haze and underwater, is depicted in Fig. 4 and Fig. 5, respectively.

2.1.4 Transient Particulate Degradations

This refers to degradations caused by discrete, moving particles that pass through the camera’s line of sight only briefly. For example, rain and snow are weather-induced degradations that, unlike haze, involve transient particles that cause visible streaks, flicker, or occlusions across video frames. While haze is primarily caused by the scattering of light due to aerosols suspended in the atmosphere, rain and snow degrade video quality through the direct interaction of falling particles with the camera’s line of sight. These effects are dynamic, spatially non-uniform, and temporally inconsistent, making them distinct from haze and often addressed separately in the literature [31]. In contrast, haze generally produces a veiling glare that reduces contrast, biases color, and obscures fine scene details.



Fig. 6: An example of two levels of real low-light video degradation: normal light, light intensity at 20% and 10%; video frames from BVI-lowlight dataset [32]

2.1.5 Complex Degradations

In real-world scenarios, videos are often affected by multiple degradation factors simultaneously. For instance, videos captured in low-light environments typically suffer from under-exposure, low contrast, and significant noise. Limited photon availability results in dark images where details are obscured in shadows. To compensate, cameras may increase exposure time, risking motion blur, or raise sensor gain (ISO), which introduces noise. Consequently, low-light videos commonly exhibit a combination of issues: low brightness, poor contrast, color shifts from white balance errors, and amplified noise. Fundamentally, these degradations stem from a low signal-to-noise ratio (limited light leads to weak pixel intensities and relatively high noise levels). Camera post-processing that brightens the image also amplifies noise. Moreover, automatic exposure adjustments occurring frame-by-frame often cause temporal instability, resulting in flickering or stalled appearance. The combined effect of noise, motion blur, quantization artifacts, and temporal fluctuations makes low-light video enhancement a particularly challenging task that demands a careful trade-off between noise suppression and detail preservation. An example of low-light footage is shown in Fig. 6.

Another example is atmospheric turbulence condition which involves distortions such as fog or haze, which reduce image contrast, and turbulence caused by temperature variations or aerosols. The increase in temperature difference between the ground and air manifests as changes in the interference pattern of refracted light. Under strong turbulence, video imagery suffers not only from blurring and scintillation, which is small-scale intensity fluctuations, but also from shearing effects, where different parts of objects appear to move in different directions. This complex degradation is commonly referred to as heat haze, with an example shown in Fig. 7.

2.2 Traditional Video Enhancement and Restoration Methods

We refer to non-learning-based methods as traditional methods. Traditional video restoration and enhancement techniques can be broadly categorised into model-driven and rule-based approaches, depending on their underlying design principles. Model-driven methods incorporate prior knowledge about the video acquisition process, noise characteristics, or motion dynamics, and are often inspired by perceptual models of human vision. Notable examples are Retinex theory for low-light enhancement or atmospheric scattering degradation model (Eq. 2). Another common approach involves constructing objective functions composed of a fidelity term and regularization terms



Fig. 7: An example of two levels of atmospheric turbulence video degradation

Table 1: Common video degradations and their characteristics.

Degradation	Primary Causes	Key Characteristics
Blur	Relative motion (camera/object) during exposure; long exposure, defocus, atmospheric blur	Loss of sharpness, streaking and smear, detail loss; varies per frame and spatially
Noise	Sensor physics (photon shot, read, thermal and dark current noise, high ISO gain) quantization, transmission	random intensity/color variations; mostly spatially independent but can be low frequency; mostly temporally uncorrelated; causes loss of fine details and adds undesired texture
Transient particulate degradations	Precipitation particles crossing the line-of-sight	Bright/dark streaks or blobs; transient, spatially sparse occlusions; temporally inconsistent, causing flicker
Continuous Scattering Degradations	Atmospheric (dust, smoke, fog) or water particles scattering/absorbing light	Low contrast, white/gray veil over entire frame; global light color cast; tends to be depth-dependent; temporal changes tied to weather/ambient conditions or camera motion through environment
Low-Light	Insufficient illumination; short exposure; small aperture	Dark frames with low contrast and color distortion; high noise due to low SNR; auto exposure changes cause flicker; potential motion blur with higher exposures; details hidden in shadows
Atmospheric Turbulence	Refractive-index fluctuations from temperature gradients or aerosols over long paths	Geometric distortions (warping, shearing), local blur and scintillation; strong temporal variation; reduces sharpness and contrast

that encode natural image priors (e.g., local smoothness, non-local similarity, and sparsity). These optimization problems are typically solved using iterative convex optimization methods such as ADMM [33]. These model-based methods offer principled formulations and are often interpretable, making them appealing in contexts where explainability is important.

In contrast, rule-based methods enhance video quality using predefined, often hand-crafted rules, without explicitly modeling the underlying image formation process or human visual perception. Common examples include global histogram equalization, fixed gamma correction, linear contrast stretching, and brightness scaling. Tone mapping is also frequently implemented in this manner, using static curves or compression functions such as logarithmic or sigmoid mappings. These methods typically apply the same transformation uniformly, regardless of scene content. While this makes them computationally efficient and straightforward to implement, their lack of adaptability limits their effectiveness in handling diverse or complex video conditions.

Different image processing methods have been developed to address specific forms of degradation. For instance, noise in images and videos has been traditionally addressed through spatial, temporal or spatio-temporal filtering. The early spatial filtering techniques including median, Gaussian and Wiener filter [34, 35] are computationally efficient but suffer from severe blurring and loss of fine details. They also do not utilise temporal information inherent in video sequences. Temporal filters, on the other hand, exploit the redundancy present in consecutive frames [36–38]. However, they can introduce artifacts and blur and are efficient only in relatively static videos. Spatio-temporal methods are aiming to combine the strengths of both approaches, utilising information both in spatial and temporal domains. Statistical filters such as extensions of Wiener and Kalman filters can be applied only under specific assumptions (such as stationarity, linearity or normality of the process) which in the case of real world videos rarely hold. Another example of spatio-temporal filtering approach is extensions of BM3D (Block Matching and 3D filtering) [39] for videos that searches for similarities across frames [40–42]. These methods tend to outperform early filtering techniques, however, they have high computational complexity, can introduce block artifacts and their performance of these methods falls short in high noise level scenarios.

Traditional video dehazing methods often rely on atmospheric scattering model which describes hazy images as a combination of attenuated scene radiance and atmospheric airlight (see Eq. 2) [43]. The techniques based on Dark Channel Prior (DCP) [44, 45] assume that most outdoor images have at least one color channel with very low values in the areas excluding sky. Methods utilising this assumption have been proposed for images [43, 46, 47] and videos [48–50]. However, DCP struggles in scenes with high brightness and with large sky areas, causing color distortion and incorrect estimation of transmission map. Applying methods suited for images to video frames causes flickering and temporal inconsistencies.

Conventional deblurring techniques aim to invert the blurring process that is mathematically modelled as convolution of a sharp image with Point Spread Function (PSF). They address it via deconvolution (e.g. Wiener deconvolution [51] or Richardson-Lucy deconvolution [52]). However, these methods require a known PSF

and assumptions about noise and signal that do not necessarily hold. Additionally, if PSF is inaccurately estimated, they can introduce artifacts such as noise and residual blur. Blind deconvolution does not require the knowledge of PSF [53], but it often struggle with accurate frame alignment and separating motion blur from the actual movement.

Traditional methods for atmospheric turbulence mitigation rely on so called “lucky regions” or “lucky images” — the cleanest and sharpest frames or frame regions that appear in a video sequence due to changing nature of atmospheric turbulence [54, 55]. These frames are then aligned and fused to produce a clearer image. These techniques are only efficient for scenes with little or no motion as it is difficult to distinguish between the turbulence and genuine motion at the registration stage. The same limitations apply to multi-frame fusion techniques [56, 57].

For conventional low-light enhancement, histogram-based methods like Histogram Equalisation (HE) and its improved adaptive modifications, Adaptive Local Histogram Equalization (ALHE) [58] and Contrast Limited Adaptive Histogram Equalization (CLAHE) [59] were introduced. They involve manipulations with histograms that are aimed at improving global contrast, however they can result in over-enhancement and in case of CLAHE might introduce noise, result in loss of detail and blocky artifacts.

Based on models of human vision, Retinex theory [60] states that an image $I(x, y)$ can be decomposed into two components: illumination $L(x, y)$ and reflectance $R(x, y)$, using the relation $I(x, y) = L(x, y)R(x, y)$. This model assumes that intrinsic properties of the scene (such as color and texture) come from reflectance component, while most undesirable brightness variations stem from illumination, which can be estimated and suppressed to enhance local contrast and reveal finer details. Traditional low-light enhancement is achieved by estimating and boosting illumination component while preserving and enhancing the reflectance component. Building upon this theoretical framework, LIME [61] estimates illumination through minimization of an objective function incorporating a structure-aware L1 smoothness prior. Single-scale Retinex (SSR) methods typically use Gaussian filter to estimate the illumination component from the input image [62]. The Multi-Scale Retinex methods [63] combine the results from SSRs at different scales that ensure better dynamic range compression and enhancement results.

Traditional video restoration and enhancement methods, while being foundational to the field, share common limitations: their strong reliance on specific hand-crafted priors or explicit models that may not hold universally and often fail in the conditions of severe degradations. They are relying on careful parameter tuning, struggle with dynamic scenes and tend to introduce artifacts and new degradations. These limitations has driven interest towards data-driven approaches. They can learn to distinguish noise from signal and model complex scene motion without pre-defined rules, shifting video enhancement from explicit modelling to implicit learning of degradation from the data.

2.3 Supervised Deep Learning Based Video Restoration and Enhancement Techniques

Compared to traditional video restoration and enhancement methods, supervised deep learning models can implicitly learn more sophisticated representations and capture complex priors directly from data. This capacity for end-to-end learning has made supervised deep learning the dominant paradigm in a wide range of applications, including video restoration and enhancement.

A number of recent surveys have comprehensively reviewed supervised deep learning approaches for video restoration and enhancement, covering tasks such as video denoising [64], deblurring [65], dehazing [66], low-light enhancement [67–69], deraining [70], and atmospheric turbulence mitigation [71]. Broader overviews of supervised techniques across multiple video restoration tasks are also provided in [14, 72]. These surveys offer valuable context on the evolution and current state of supervised video restoration and enhancement methods. Readers are referred to these works for scenarios where paired ground truth data is available or synthetic data is used for supervised training.

2.3.1 Convolutional Neural Networks

Convolutional Neural Networks (CNNs) are foundational for many video restoration techniques because of their spatial feature extraction capabilities. Common CNN-based approaches use encoder-decoder structures like UNet [73] or stacked convolutional layers. Temporal processing in CNNs can involve sliding windows, 3D convolutions, or explicit motion estimation and compensation via optical flow, though some methods avoid explicit motion estimation for efficiency.

A key example is FastDVDnet ([74] for real-time video denoising without explicit motion estimation. It uses a UNet backbone with interleaved spatial and temporal convolutions on a sliding window of frames, demonstrating effective temporal feature aggregation without the high computational cost of optical flow. Another notable CNN method is RViDeNet [75], for supervised raw video denoising, which also introduced the CRVD benchmark dataset. It processes raw Bayer pattern video by packing it into four sub-sequences, denoising each using deformable convolutions for alignment and non-local attention, then fusing the results and using an ISP module for sRGB output.

CNNs are also widely used for video deblurring and video dehazing. For instance, PDVD uses a multi-stage CNN for video dehazing where attention-based UNets align and fuse neighbouring frames, followed by a residual-attention UNet for final dehazing [76].

The evolution of CNN methods shows a trend towards more sophisticated temporal modeling, incorporating elements like deformable convolutions and attention mechanisms.

2.3.2 Recurrent Neural Networks

Recurrent Neural Networks (RNNs), including Long Short-Term Memory (LSTM) and Gated Recurrent Units (GRUs), are well-suited for sequential video data, modeling temporal dependencies and propagating information across frames for temporal

consistency. They typically process frames sequentially, maintaining an internal state. Bidirectional RNNs, processing sequences in both forward and backward directions, are common for video restoration.

BasicVSR [77] and its successor BasicVSR++ [78] are prominent RNN-based methods, primarily for Video Super-Resolution (VSR), with BasicVSR++ also applied to compressed video enhancement and real-world VSR. BasicVSR established a framework with Propagation, Alignment, Aggregation, and Upsampling modules. BasicVSR++ enhanced this with second-order grid propagation to allow more extensive bidirectional propagation and relaxes the first-order Markov assumption, improving information flow, especially in occluded regions and with flow-guided deformable alignment that uses optical flow to guide Deformable Convolution Network (DCN) offset learning, improving training stability and alignment effectiveness. These models set the benchmark in recurrent models for video enhancement. Another example is Frame-Consistent Recurrent Video Deraining (FCRVD) [79], that uses a two-stage recurrent network. The first stage estimates an initial rain-free frame, guiding the second stage’s refinement using previous frames. It employs a two-stage recurrent network: the first stage estimates an initial rain-free frame from a single input, which then guides the second stage in refining the result using information from previously restored frames. A key innovation is its dual-level flow-based regularization (at coarse flow and fine pixel levels) designed to maintain motion consistency, directly contributing to temporally coherent deraining.

2.3.3 Transformer-Based Networks

Transformer models, with their self-attention mechanisms, excel at capturing long-range dependencies in video sequences, potentially outperforming CNNs with limited receptive fields and RNNs with sequential processing bottlenecks. Challenges include managing computational cost and adapting self-attention to video data.

The Video Restoration Transformer (VRT) [80] is a versatile model for VSR, deblurring, denoising, and more, with over 1258 citations. Its multi-scale architecture employs Temporal Mutual/Reciprocal Self Attention (TMSA/TRSA) that is applied on video clips for joint motion estimation, feature alignment, and fusion, with standard self-attention for intra-clip feature extraction. Parallel Warping uses information from neighboring frames while Shifted Window Mechanism enables cross-clip interactions by cyclically shifting the video sequence. VRT allows parallel frame prediction and models long-range temporal dependencies effectively. Transformers address RNN limitations like gradient issues in long sequences and CNN receptive field restrictions. VRT’s TMSA/TRSA are specifically designed for joint motion estimation, alignment, and fusion, highlighting the need for video-specific attention mechanisms. Computational cost remains a challenge, addressed by innovations like VRT’s multi-scale design and clip-based processing.

3 Unsupervised Learning in Video Restoration and Enhancement

Unsupervised methods reduce the reliance on labor-intensive data collection and annotation, helping to address the limitations posed by the scarcity of paired training data, particularly for dynamic scenes captured under adverse conditions or affected by complex, poorly understood degradations. Models trained on diverse unlabelled data often develop representations that are more robust to content and degradation variability than their supervised counterparts. These approaches are especially favourable in cases where degradation processes are poorly understood or difficult to simulate or characterise. By learning directly from the input data, they can adapt to the unique properties of each video, making them well suited for in-the-wild enhancement tasks.

3.1 Unsupervised, Self-Supervised, and Zero-Shot Learning for Video Tasks

In video restoration and enhancement, unsupervised learning refers to training models on video sequences without corresponding clean ground truth. The goal is to learn the statistical properties of clean video content or to model the degradation process directly from unlabelled data. This can involve generative models, such as generative adversarial networks (GANs) and diffusion models (DMs), or using frameworks that exploit inherent video structures (e.g. temporal consistency), or methods that discover low-dimensional representations or structural patterns in the data.

Self-supervised learning is considered a subset of unsupervised learning in which the supervision signals are derived automatically from the data itself. This is achieved through the design of *pretext tasks* [81] — auxiliary learning objectives that encourage the model to learn useful representations for downstream tasks such as restoration or enhancement. Common pretext tasks include predicting missing or corrupted regions of a frame based on surrounding context, enforcing consistency between different augmented views of the same video, and maintaining cycle-consistency between domain-translated video pairs (e.g., between domains A and B).

Zero-shot learning (ZSL) addresses scenarios where no task-specific training data is available at test time. In video restoration and enhancement, this typically involves leveraging pre-trained models as priors or adapting directly to the degraded input by exploiting internal signal statistics or known degradation models. ZSL aims to handle previously unseen or unlabelled degradations without the need for retraining, making it particularly suitable for real world or domain-agnostic applications. Although ZSL is conceptually distinct from unsupervised and self-supervised learning, the boundaries between them often blur in practice in the field of image and video enhancement. Recent works frequently use these terms interchangeably, especially when models exploit internal priors or learn from observed data like distorted video sequences.

In the following sections, we classified the existing unsupervised, self-supervised and zero-shot video enhancement techniques broadly into 5 broad categories: (1) domain translation with unpaired learning, (2) self-supervised signal design, (3) consistency-based methods, (4) degradation-aware methods and (5) prior-based methods. We mention representative works and their contributions in each category.

3.2 Domain Translation with Unpaired Learning

Unpaired adversarial training is a common strategy to bridge the domain gap between degraded and clean videos. They learn a mapping from degraded to clean domains without paired examples, typically via *cycle-consistency* and *adversarial objectives*. Cycle-consistency frameworks, inspired by CycleGAN [82], employ dual-generator architectures to enforce content preservation: a generator G maps low-quality video frames to high-quality outputs, while an inverse generator F attempts to reconstruct the original input from the enhanced output. This cycle-consistency constraint ensures that the restored frames retain the original content, even in the absence of paired ground truth.

An adaptation of the CycleGAN structure has been proposed for low-light enhancement in [83], where the brightness and color characteristics of a low-light video (domain A) are mapped to those of a reference frame (domain B). Fuoli et al. [84] propose an adversarial framework, comprising a lightweight recurrent generator to propagate spatio-temporal information across frames, a degrader network with the same architecture, and a single joint recurrent discriminator that evaluates the realism of the enhanced video. By enforcing adversarial loss, the generator learns to produce outputs with both natural textures and temporal coherence. Similarly, Patil et al. [85] address real-world video dehazing in an unpaired setting by coupling a dehazing network with a haze synthesiser. Their architecture integrates a Mixed Multi-Level Attentive (MMA) module for robust feature extraction and a Recurrent Multi-Attentive (RMA) module for temporal alignment, all within a compact 1.8M parameter model. The network learns to remove haze from input videos and reintroduces it via a backward branch, with a cycle-consistency loss enforcing structural preservation between the original and re-hazed frames.

Another example is LightenFormer, proposed by Lv et al. [86], the first unsupervised transformer-based approach for low-light video enhancement. Unlike Retinex-based methods, LightenFormer does not explicitly decompose images into illumination and reflectance. Instead, it adopts an S-curve adjustment strategy commonly used in professional image editing, implicitly capturing illumination cues by focusing on the darkest regions and amplifying them. Its spatial-temporal self-attention mechanism models long-range dependencies both within and across frames, allowing the network to aggregate contextual information for effective denoising. Trained on unpaired datasets (collections of low-light and normal-light videos), using cycle-consistency and adversarial losses, LightenFormer learns to enhance illumination and recover details. The resulting improvements in brightness and perceptual quality are comparable to those achieved by methods relying on explicit priors, yet are obtained through the network’s internal representation learning.

Diffusion Models (DMs) have also been applied to domain translation tasks using cycle-consistency constraints. However, because they rely on training two generators and require large amounts of training data, DM-based methods have so far been primarily developed for images rather than videos [87].

3.3 Self-Supervised Signal Design

Self-supervised signal design techniques obtain their loss functions from the properties, transformations or inherent structure of degraded input data itself. These methods do not rely on external datasets or domain discriminators; instead, they exploit internal redundancies and constraints within the data.

3.3.1 Blind-Spot and Noise-Based Methods

When enhancing videos degraded by noise, a key challenge is learning from the noisy data alone. *Blind-spot networks* have emerged as a powerful self-supervised tools for this scenario. They are designed such that when predicting a pixel’s intensity, the network has no access to that specific pixel in the input, relying only on its neighbors. This prevents the network from trivially copying the noisy input value, forcing it to learn denoising from context.

Sheth et al. [88] introduced an Unsupervised Deep Video Denoiser (UDVD) that extends the blind-spot principle to the video domain. Their CNN is trained exclusively on noisy videos by masking out each target pixel and relying on adjacent pixels across spatial and temporal neighborhoods to predict it. By randomly shifting input frames or using multiple noisy frames of the same scene, UDVD obtains supervision signals similar to Noise2Noise [89], effectively treating one noisy observation as the target for another. This approach achieved denoising performance close to supervised methods on various real-world datasets, despite never seeing a clean video. A crucial benefit of the video setting is redundancy: even though any single pixel is noisy, neighboring frames often carry a slightly different noise realization for the same scene point, which the network can exploit. UDVD and similar blind-spot methods demonstrate that, given sufficient video data, a model can calibrate itself to remove noise without ground truth, learning the noise distribution in the process.

Building on this idea, Dewil et al. [90] proposed Multi-Frame2Frame (MF2F), a self-supervised blind training scheme for multi-frame video denoising that also performs noise level estimation. In their approach, the network is trained to map a stack of consecutive noisy frames to a denoised output for the central frame. By assuming the noise is uncorrelated across frames, any one frame can serve as a target for its neighbors. In practice, they employ a strategy where one frame is reconstructed from its adjacent frames (which are treated as references); the loss penalises differences between the network’s output and the actual noisy target frame. Since the only consistent signal across frames is the true underlying image (noise is random), the network learns to recover that image while the noise averages out. Furthermore, MF2F integrates a noise estimation sub-task. The network learns the noise variance by predicting inter-frame differences, which facilitates adaptive filtering of varying (heteroscedastic) noise levels. This blind, self-supervised joint denoising and noise-level learning yields a robust video denoiser that requires no clean data, effectively learning the noise model directly from the input video sequence itself.

While blind-spot methods avoid using the target pixel, they can suffer from information loss since masked pixels are never directly seen. Wang et al. [91] address this limitation by proposing a recurrent self-supervised denoising framework with a

Richer and Denser Receptive Field (RDRF). Their method fully exploits both the reference frame and neighboring frames by aggregating information from a larger spatio-temporal neighborhood, while adhering to the blind-spot constraint. RDRF employs a recurrent architecture that processes a video in both forward and backward directions, integrating information from distant frames to enlarge the temporal receptive field. A key innovation is a training scheme that maintains the self-supervised mask constraint even in a recurrent setup (which is non-trivial, as naive recurrence could leak a pixel’s own information from one time step to the next). This is achieved through offset blind-spot masks and merge features from multiple timesteps, ensuring that each output pixel is influenced by many context pixels, including those from past and future frames, but never by itself at the same timestep. The result is improved detail preservation and lower noise, as the network can utilise more of the video’s content. Empirically, RDRF outperforms earlier blind-spot video denoisers, achieving cleaner results with fewer texture artifacts, thanks to its denser utilization of available data.

Recently, a SpatioTemporal Blind-spot Network (STBN) [92] has been proposed to enhance video denoising through bidirectional blind-spot feature propagation, ensuring accurate temporal alignment without leaking target pixel information. To address the instability of motion estimation in noisy conditions, the framework incorporates an unsupervised optical flow distillation mechanism, which guides the learning of flow from noisy videos using enhanced outputs. Furthermore, STBN replaces conventional bilinear interpolation in the warping operation with nearest-neighbor interpolation, which better preserves spatial correlations and the original noise distribution.

As shown in Tables 2 and 3, the STBN consistently shows the best PSNR/SSIM scores across every noise level on both synthetic noise datasets Set8 and DAVIS when compared with other blind-spot unsupervised approaches.

Method	$\sigma=10$	20	30	40	50	Avg
MF2F [90]	36.01 / 0.9379	33.79 / 0.9115	32.20 / 0.8831	30.64 / 0.8413	28.90 / 0.7775	32.31 / 0.8703
UDVD [88]	36.36 / 0.9510	33.53 / 0.9167	31.88 / 0.8865	30.72 / 0.8595	29.81 / 0.8349	32.46 / 0.8897
RDRF [91]	36.67 / 0.9547	34.00 / 0.9251	32.39 / 0.8978	31.23 / 0.8725	30.31 / 0.8490	32.92 / 0.8998
STBN [92]	37.24 / 0.9594	34.41 / 0.9322	32.76 / 0.9072	31.57 / 0.8837	30.62 / 0.8608	33.32 / 0.9087

Table 2: Performance comparison of unsupervised blind-spot methods [91, 92] (Set8 dataset, PSNR/SSIM values)

Method	$\sigma=10$	20	30	40	50	Avg
MF2F [90]	38.04 / 0.9566	35.61 / 0.9359	33.65 / 0.9065	31.50 / 0.8523	29.39 / 0.7843	33.64 / 0.8871
UDVD [88]	39.17 / 0.9700	35.94 / 0.9428	34.09 / 0.9178	32.79 / 0.8949	31.80 / 0.8739	34.76 / 0.9199
RDRF [91]	39.54 / 0.9717	36.40 / 0.9473	34.55 / 0.9245	33.23 / 0.9032	32.20 / 0.8832	35.18 / 0.9260
STBN [92]	40.35 / 0.9613	37.67 / 0.9606	36.00 / 0.9454	34.73 / 0.9296	33.70 / 0.9138	36.49 / 0.9451

Table 3: Performance comparison of unsupervised blind-spot methods [91, 92] (DAVIS dataset, PSNR/SSIM values)

3.3.2 Optimization-Unrolling Methods

Optimization-unrolling methods treat image and video enhancement as an inverse problem and solve it with an iterative optimiser (e.g. ADMM [33]), “unrolling” those iterations into a trainable network whose blocks represent an optimization step. During the training, the loss function is composed of the optimiser’s internal data-fidelity term and handcrafted regularisers. A number of methods based on unrolled optimisation were developed for image enhancement [93, 94].

UDU-Net [95] unrolls the optimization process into a deep network that decomposes the video signal into spatial and temporal factors, which are then updated iteratively. The spatial component (Intra-subnet) corrects exposure and contrast using priors inspired by expert photography adjustments, effectively learning a mapping towards well-exposed statistics such as histograms of professionally retouched images. A human perceptual feedback mechanism is also incorporated to prevent under- or overexposure, giving the user some control over the brightness level. The temporal component (Inter-subnet) ensures that the illumination changes are smooth over consecutive frames. A discriminator is incorporated to ensure that the enhanced videos match the illumination distribution of expert-retouched footage. Experimental results demonstrate that UDU-Net outperforms previous unsupervised learning methods by more than 3dB in PSNR on the SDSD [96] dataset.

3.3.3 Deep Plug-and-Play

Deep Plug-and-Play (PnP) is a hybrid framework that integrates deep learning with classical optimization techniques, such as those used in model-based approaches for solving inverse problems [97]. Specifically, it replaces the prior term in an optimization problem with a pre-trained image denoiser. The motivation behind PnP is to combine the advantages of both model-based and learning-based approaches. Model-based restoration methods are task-agnostic, relying on a specified degradation operator H in the formulation $I_{\text{obv}} = HI_{\text{idl}} + n$ (Eq. 1), and do not require training, making them adaptable across tasks. However, they depend on hand-crafted priors, and they are typically slower as it solves the problem with iterative algorithm, like ADMM [33] or FISTA [98]. In contrast, learning-based methods require extensive training but offer fast inference and strong performance due to end-to-end optimization. Hybrid approaches, such as deep plug-and-play methods, combine the strengths of both paradigms by using learning-based denoisers as learned priors within iterative model-based frameworks.

PnP is not exactly a form of learning, but rather an unsupervised inference or optimization framework that can incorporate learned components. The classic optimization form is given by

$$\min_x \frac{1}{2} \|Ax - I_{\text{obv}}\|^2 + \lambda R(x), \quad (3)$$

where x is an estimate of the ideal image I_{idl} , λ controls the trade-off between the data fidelity term $\frac{1}{2} \|Ax - I_{\text{obv}}\|^2$ and the regularization term $R(x)$, which serves as a prior. In PnP, the proximal operator associated with $R(x)$ is replaced by a pretrained

denoiser. For applications in image restoration and enhancement, we refer the reader to [99, 100] for more details.

For video restoration and enhancement, Yuan et al. [101] adopt a PnP-ADMM framework, leveraging FastDVDnet [102], a deep video denoising network, as the learned prior. Zerva et al. [103] similarly employ a PnP-ADMM strategy but incorporate DnCNN [104], a pretrained image denoiser, alongside optical flow for motion compensation. Their approach primarily aims for video super-resolution. While deep PnP frameworks offer flexibility and strong generalization, they remain less popular in practice compared to standard image restoration networks due to their inherently iterative nature, which results in slower inference and increased computational cost.

3.4 Consistency-Based Methods

Consistency constraints in video restoration force stable outputs across video frames or semantics. Methods based on consistency enhance video by enforcing agreement across related signals, such as neighbouring frames or semantic content. Temporal consistency ensures smoothness across time, typically by penalising differences between frames after motion compensation. Semantic consistency uses a pretrained model to preserve high level features such as object identity or segmentation across enhancement. Consistency losses act as regularisers and are usually complemented by priors or data-fidelity terms.

3.4.1 Temporal consistency

Unsupervised video restoration methods must ensure temporal consistency to prevent flickering or jitter across frames. Common approaches involve enforcing alignment between restored frames by accounting for motion dynamics. Lin et al. [105] propose an unsupervised flow-aligned sequence-to-sequence model (S2SVR) that explicitly integrates optical flow into the restoration process. Their framework jointly trains a video restoration network along with an in-built optical flow estimator in a self-distillation manner: the flow network, trained without ground truth flow, aligns neighboring frames to the reference frame, while the restoration network processes these aligned sequences. A distillation loss guides the flow estimator by using results of a flow estimator network, pre-trained on high-quality data, as pseudo groundtruth, effectively providing feature alignment and addressing the data discrepancy between low-quality and high-quality videos. By obtaining more reliable motion correspondence on degraded videos, the S2SVR can aggregate information from multiple frames without blurring moving objects, improving deblurring, super-resolution, and compression artifacts removal. Similarly, Yeh et al. [106] enforce temporal consistency in a zero-shot manner using a hierarchical latent warping strategy. Their DiffIR2VR-Zero framework applies a pre-trained diffusion-based image restoration model in frame-wise fashion, while introducing intelligent warping of latent features between keyframes and their neighboring frames to maintain coherence. By combining optical flow with feature matching in a hybrid token merging mechanism, they adapt static image restoration model to video, achieving significantly improved temporal stability without retraining. Instead of estimating motion flow, Varghese et al. [107] estimate depth from two

consecutive frames and use view synthesis to enhance temporal consistency. However, since this work focuses on underwater enhancement, the estimated depth is also used to compute the light transmission map.

An alternative strategy is to incorporate recurrent or plug-in temporal modules into an image restoration network. Fu et al. [108] present *Temporal-as-a-Plugin* (TAP), an unsupervised video denoising framework that inserts tunable temporal filtering blocks into a pre-trained single-frame denoiser. By fine-tuning these temporal modules on the target video data, TAP utilises inter-frame information to denoise consistently across time. A progressive training schedule is used, where initial frame-by-frame denoising produces pseudo-clean frames, which are then used to iteratively refine the temporal modules, improving the network’s performance on real videos without any ground truth.

3.4.2 Semantic consistency

Zheng et al. [109] propose a Semantic-Guided Zero-shot (SGZ) method for low-light video enhancement. Their SGZ framework uses a pre-trained object recognition or segmentation network to enforce semantic consistency between low-light and enhanced frames. The key is the semantic content of a frame should remain invariant under enhancement. The SGZ network is optimised to maximise the similarity of deep semantic features extracted from the original and enhanced frames, and simultaneously improve the confidence of object detections in the enhanced output. By treating the original and enhanced frames as two views of the same scene, SGZ ensures that the network does not introduce artifacts that alter content. This method effectively performs high-level contrastive alignment.

3.5 Degradation-Aware Methods

These approaches simulate or estimate the degradation process and re-degrade intermediate outputs during training, aligning the network’s objective with real-world noise characteristics.

3.5.1 Degradation Simulation and Re-Degradation

Another category of unsupervised methods derives self-supervision from simulating the degradation process and enforcing reconstruction consistency, often referred to as “analysis-by-synthesis”. The core idea is to apply a differentiable degradation model to the restored output and compare it against the original input, thereby generating a training signal in the absence of ground truth. A representative example is Reblur2Deblur [110], which addresses video deblurring using a physics-based motion blur model. After restoring a sharp frame, the output is reblurred using a blur kernel estimated from optical flow between consecutive frames. A self-supervised loss minimises the discrepancy between this reblurred result and the original blurry input, enforcing physical consistency with the observed motion. However, this method is not fully unsupervised, as it relies on a supervised pre-trained image or video deblurring network and uses a hybrid loss function during fine-tuning, which combines the self-supervised loss with a supervised loss to avoid degenerate solutions.

Similar analysis-by-synthesis strategies have been applied to other video degradation types. In the context of denoising, this involves reintroducing noise to the denoised output and compare it against the original noisy input. Lee et al. [111] follow this principle in their “Restore-from-Restored” (RFR) approach for self-supervised video denoising. This method is based on Noise2Noise [89] and is an extension of frame-to-frame training approach [112] that allows the network to train during the test phase with self-supervision. RFR does not require optical flow estimation due to translation equivariant property of Fully Convolutional Networks (FCNs). A pre-trained denoiser is used to generate a pseudo clean video from a given noisy input, forming synthetic training pairs of {noisy frame, pseudo-clean frame}. The denoiser is then fine-tuned by reintroducing noise to its output and minimising the error to the input. This process effectively treats the network’s own output as a pseudo ground truth, refining the model in offline or iterative manner.

In [113], Zheng et al. use an untrained deep network that requires only the single test noisy video for its training process. A core contribution is the development of a self-supervised loss function, an extension of the “Recorrupted-to-Recorrupted (R2R)” idea for images and videos (ER2R and VER2R). This loss function works by re-corrupting the noisy input frames with additionally simulated noise (from the same distribution as the measurement noise) to generate training pairs. This re-degradation scheme allows the loss to act as an unbiased estimator of its supervised counterpart, making it applicable to general random noise beyond just Gaussian noise. The method employs a two-stage training approach: first, a spatial denoising module is pre-trained using the ER2R loss to facilitate frame alignment; subsequently, the entire video denoising network, which includes a motion-compensation module and a lightweight temporal attention module for fusing temporal neighbors and handling misalignments, is trained using the VER2R loss.

3.6 Prior-Based Methods

In prior-based methods, the enhancement is regularised with explicit knowledge (unlike consistency or self-supervised signal design methods, where supervision stems from implicit information within the signal), that is inspired by the physics models of image formation or learned priors distilled from large datasets. Priors are aimed to reduce artefacts, impose desirable properties and guide plausible reconstructions.

3.6.1 Physics-Based Priors

In the absence of ground truth, integrating domain-specific physics models or priors can meaningfully constrain the solution space for video restoration. Two prominent examples are atmospheric scattering models for dehazing and the Retinex theory for low-light enhancement.

As discussed in 2.2, Retinex theory states that an image can be decomposed into reflectance and illumination. Low-light video enhancement thus involves estimating and adjusting the illumination while preserving reflectance. Several unsupervised methods incorporate this idea or related illumination priors. For instance, Zero-TIG [114], a zero-shot learning approach designed for enhancing low-light and underwater

videos, exemplifies this principle by decomposing input frames into reflectance and illumination components for targeted enhancement. The architecture features two main modules: an enhancement module and a temporal feedback module. Similar to Zero-IG [115], the enhancement module contains three subnetworks: a low-light denoising network (LD-Net), trained via self-supervision following Noise2Noise [89]; an illumination estimation network (IE-Net); and a reflectance denoising network (RD-Net). To ensure temporal consistency, the feedback module recursively integrates information from previously enhanced frames. This is achieved by applying histogram equalisation to the current pre-denoised frame, estimating optical flow via RAFT between the previous and current frames, and warping the enhanced components of the previous frame to align with the current frame before reintegration. Optimisation is driven by a set of 11 no-reference loss functions adapted from prior zero-shot methods. For underwater video enhancement, Zero-TIG further addresses colour distortion by adaptively balancing RGB channels during illumination estimation.

In dehazing problems, several priors are commonly employed, including the colour ellipsoid prior, colour line prior, dark channel prior, colour attenuation prior, and haze line prior. These priors are detailed in comprehensive reviews of single-image defogging [116]. However, the extension of unsupervised dehazing or defogging techniques to video remains limited and relatively underexplored.

3.6.2 Learning-based Priors

As an alternative to using known physics-based or image formation models, deep neural networks have been employed to capture low-level image statistics as implicit priors, a concept first introduced in the Deep Image Prior (DIP) framework [117]. Subsequently, Deep Generative Prior [118] was proposed, where image priors are learned by a GAN trained on large-scale natural images, rather than optimising a single low-quality image as in DIP. More recently, DDRM [119] employs diffusion generative models as learned priors, using a variational inference objective to estimate the posterior distribution of the inverse problem. In unsupervised settings, priors based on deep neural networks have demonstrated impressive empirical results across a variety of image restoration tasks. For instance, UnDIVE [120] introduces a generative prior trained on underwater images using Denoising Diffusion Probabilistic Models (DDPM) [121]. Similarly, UPID-EDM [122] leverages visual-language priors embedded within the Contrastive Language-Image Pre-training (CLIP) model [123]. The CLIP-based priors assist in distinguishing between rainy and clean images.

Applying learning-based priors designed for images to video enhancement tasks often results in flickering artefacts across frames. To address this issue, Shrivastava et al. proposed the Video Dynamics Prior (VDP) [124], which employs two networks, f and g : one predicts the latent embedding of the next frame based on the current frame’s embedding ($z_{t+1} = g(z_t)$), while the other reconstructs the video frame \hat{X}_{t+1} from the predicted latent space, $\hat{X}_{t+1} = f(z_{t+1}) = f(g(z_t))$. To the best of our knowledge, this is only one work on video enhancement that uses a learning-based prior.

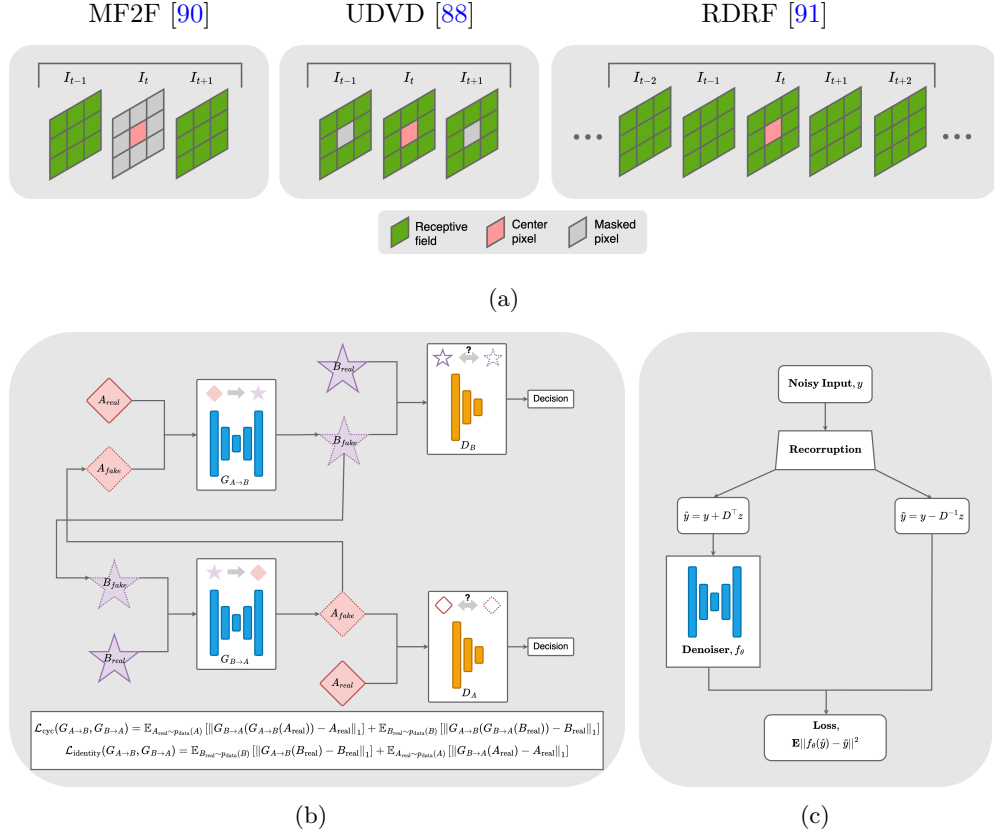


Fig. 8: Key design concepts in recent unsupervised video-enhancement pipelines. (a) Spatio-temporal receptive fields. Heat maps compare the effective receptive field over a multi-frame window for MF2F, UDVD, and R2RF: MF2F’s motion-aligned warping draws information from closest frames; UDVD’s convolutions focus on locally-aligned motion edges; R2RF’s recursive diffusion has the broadest coverage. (b) CycleGAN backbone. Two generators $G_{A \rightarrow B}, G_{B \rightarrow A}$, and two discriminators D_A, D_B are tied together by cycle-consistency and identity losses, enabling translation between domains A and B without paired ground truth. (c) Recorrupt-to-Recorrupt (R2R) training loop. The method involves generating two uncorrelated re-corrupted versions of the same input and learning to map one to the other, mimicking supervised denoising without clean targets.

4 Loss Functions for Unsupervised Video Restoration and Enhancement

The loss function plays a central role in deep learning by quantifying the discrepancy between predicted and target outputs, serving as the objective that guides model optimization. It provides the feedback signal for updating parameters via gradient-based

Table 4: Summary of Unsupervised Video Enhancement and Restoration Techniques

Category	Method	Key idea	Task
Unpaired Domain Translation	Fuoli <i>et al.</i> [84]	Lightweight recurrent generator-degrader pair with a joint discriminator learns spatial detail and temporal coherence through adversarial training.	Low-Light
	Patil <i>et al.</i> [85]	Compact recurrent network with MMA and RMA modules performs cycle-consistent dehazing and re-hazing.	Dehazing
	LightenFormer [86]	Unsupervised transformer model that uses an S-curve adjustment strategy instead of explicit Retinex decomposition. Trained with cycle-consistency.	Low-Light
Optimization Unrolling	UDU-Net [95]	Unrolled optimiser iteratively updates spatial (expert-photography priors + perceptual feedback) and temporal factors.	Low-Light
Deep Plug-and-Play	Yuan <i>et al.</i> [101]	PnP-ADMM framework that plugs FastDVDnet as the denoiser prior for joint video restoration/enhancement.	Denoising / Deblurring
	Zerva <i>et al.</i> [103]	PnP-ADMM with DnCNN denoiser and optical-flow compensation targets video super-resolution.	Super-Resolution
Temporal Consistency	S2SVR [105]	Jointly trains restoration and optical flow networks. Uses a pre-trained flow estimator for pseudo-groundtruth via distillation loss.	Deblurring, SR, Compression Artifacts
	DiffIR2VR-Zero [106]	Zero-shot adaptation of a pre-trained image diffusion model. Uses hierarchical latent warping with optical flow and feature matching.	General Restoration
	Varghese <i>et al.</i> [107]	Estimates depth from consecutive frames and uses view synthesis for temporal consistency.	Underwater
	TAP [108]	Inserts and fine-tunes temporal filtering blocks into a pre-trained single-frame denoiser. Uses a progressive training schedule.	Denoising
Semantic Consistency	SGZ [109]	Uses a pre-trained object/segmentation network to enforce semantic consistency between original and enhanced frames.	Low-Light
Degradation Simulation	Reblur2Deblur [110]	Re-blurs the restored frame using estimated optical flow and minimises the difference to the original blurry input.	Deblurring
	RFR [111]	Fine-tunes a pre-trained denoiser by re-adding noise to its own output (pseudo-clean frames) and comparing to the input.	Denoising
	Zheng <i>et al.</i> [113]	Uses a "Recorrupted-to-Recorrupted" (R2R) loss by adding more noise to the input frames to create training pairs for an untrained network.	Denoising
Physics-Based Priors	Zero-TIG [114]	Decomposes frames into reflectance/illumination based on Retinex theory. Uses 11 no-reference losses and temporal feedback via optical flow.	Low-Light & Underwater

Table 4: Summary of Unsupervised Video Enhancement and Restoration Techniques (continued)

Category	Method	Key idea	Task
Learning-Based Priors	VDP [124]	Learns a video dynamics prior by predicting the next frame’s latent embedding from the current one.	General Enhancement
Blind-Spot / Noise-Based	UDVD [88]	Extends the blind-spot principle to video; predicts a masked pixel using spatial and temporal neighbors from noisy frames.	Denoising
	MF2F [90]	Multi-frame blind training scheme that jointly performs denoising and noise level estimation.	Denoising
	RDRF [91]	Recurrent architecture that enlarges the spatio-temporal receptive field while maintaining the blind-spot constraint.	Denoising
	STBN [92]	Uses bidirectional blind-spot propagation, unsupervised optical flow distillation, and nearest-neighbor warping.	Denoising

methods. The choice of loss is task-specific, e.g., regression, classification, or restoration, and critically affects both convergence and generalization. Without a well-defined loss, learning would lack direction and evaluative feedback. In unsupervised learning, the design of loss functions is especially critical, as explicit ground-truth supervision is absent. Instead, learning relies on indirect signals derived from structural assumptions, internal consistency, or self-supervision. Loss functions in this setting must capture meaningful constraints, such as temporal coherence, spatial regularity, perceptual similarity, or physical consistency with degradation models. This section reviews the loss functions commonly used in unsupervised video restoration and enhancement.

4.1 Reference-Fidelity Losses

In a supervised setting, a reference-fidelity loss (sometimes also called reconstruction loss) penalises the pixel-wise difference between ground truth and network’s prediction. The most common examples are \mathcal{L}_1 (Mean Absolute Error, MAE) and \mathcal{L}_2 (Mean Squared Error, MSE) losses:

$$\mathcal{L}_1 = \frac{1}{N} \sum_{x,y} |I_{pred}(x,y) - I_{gt}(x,y)|, \quad \mathcal{L}_2 = \frac{1}{N} \sum_{x,y} (I_{pred}(x,y) - I_{gt}(x,y))^2, \quad (4)$$

where I_{pred}, I_{gt} are prediction and groundtruth correspondingly and N is the number of pixels in them.

Although being a fundamental part of supervised learning, reconstruction losses are still sometimes used unsupervised image and video enhancement in cases when the reference is created on-the-fly. For instance, in Recorrputed-to-Recorrputed adapted

for videos [113], \mathcal{L}_2 loss is calculated between a recorrputed version of an original distorted video and a network’s output calculated for a second, independently recorrputed instance of the same distorted video. In [111] conventional losses \mathcal{L}_1 and \mathcal{L}_2 are used to minimise the error between the network output and a pseudo-clean target — video frames denoised with a pre-trained denoising. Similarly, a reconstruction loss in Temporal As a Plugin (TAP) [108] minimises the pixel-wise absolute difference between the video denoiser’s output and the pseudo-clean frames created by denoising followed by re-corruption.

Reference-fidelity loss functions can provide a pixel-level guidance even in the absence of groundtruth; however, they lack absolute correctness: their performance capped by the quality of the pseudo-reference and the fidelity of the assumed corruption model.

4.2 Data Consistency Losses

A *data consistency loss* ensures that the enhanced video remains faithful to certain properties of the input video. Formally, data consistency loss explicitly penalises the discrepancy between the enhanced video frame \hat{X}_t and the input frame X_t after application of the known operator A : in its simple form, it can be written as

$$\mathcal{L}_{DC} = \|A(\hat{X}_t) - Y_t\|_p.$$

The choice of the operator A is motivated by the known imaging process and the specific degradation or transformation applied during data acquisition such as blur kernels in deblurring, optical flow in temporal alignment, or photometric curves in low-light enhancement, so that the data consistency loss faithfully enforces the physical constraints.

Depending on the type of the operator A (per-frame operator or warping that links two frames via observed motion), data consistency losses can be classified into spatial and temporal consistency losses.

4.2.1 Spatial Data Consistency Losses

Zheng et al. [109] introduce *spatial consistency loss* for low-light enhancement, that is aimed at preserving local contrast by penalising differences in the neighboring pixels’ values during enhancement. This helps to preserve edges and avoid distortion of textures.

In Zero-IG [115] and Zero-TIG [114], the self-supervised Noise2Noise-style [89] pairwise *residual and consistency loss* terms are calculated between two downsampled noisy versions of the frame, teaching the denoising subnetwork to predict and subtract noise without any clean target.

4.2.2 Temporal Data Consistency Losses

The challenging aspect of video enhancement, compared to image-based methods, is making sure the output remains free from temporal artifacts such as flickering or jitter. A common approach is to use optical flow. In UnDIVE [120], Srinath et al.

minimise the difference between the enhanced frame warped via optical flow and the enhancement of the raw frame when warped by that same flow, considering this loss in both forward and backward directions.

To ensure temporal consistency in video denoising, Dewil et al. [90] introduce multi-frame to frame (MF2F) loss which fine-tunes a video denoiser by using the previous noisy frame as a target for the current frame after applying a warping operator.

Reblur2Deblur’s unsupervised loss is computed as the pixel-wise difference between the original blurry frame and a reblurred version, that is obtained by applying a motion-based blur kernel, calculated using optical flow between adjacent deblurred frames, to the deblurred frame [110]. This, although indirectly, promotes temporal consistency and helps to avoid jitter artifacts.

Data consistency objectives keep solutions physically plausible even without references, however they offer no guidance on ambiguities the forward model cannot resolve, so results can look dull or over-smoothed unless complemented by stronger priors.

4.3 Prior-based Losses

Unsupervised video enhancing methods often include additional loss terms that encode assumptions about the desirable properties of the latent image. They can depend on additional information from other predictions, such as masks and weights. For instance, Zheng et al. [109] introduce *RGB (color) loss* is used to reduce color shifts and is calculated as a Charbonnier distance across color channels, a *brightness loss* is constrains the overall exposure of the output to a desired level and a *total variation (smoothness) loss* that sums squared spatial gradients over RGB channels is used to attenuate residual noise. Similar low-level priot-based constraints are also employed in [86] (brightness, smoothness, color) and [120] (smoothness, color).

For a high-level *semantic loss* Zheng et al. uses a segmenation network: it enforces the enhanced frame to have the same segmented structure as the original one and to preserve scene content and object boundaries.

For unsupervised low-light video enhancement, additionally to prior-based losses mentioned above, LightenFormer [86] uses two unique no-reference losses. First, an *invertibility loss* leverages the invertibility of the S-curve and ensures that enhancing then inverting a frame recovers the original, which helps to maintain image content consistency during enhancement. Second, a *noise consistency loss* exploits the assumption of noise independence between frames: it encourages the enhancement to not introduce correlated noise across frames.

Prior-based losses penalise implausible content by utilising statistical information and models of the physical process. However, hand-crafted priors are often too rigid, while learned ones can hallucinate or fail to fit data distribution, their inference is also slower due to iterative character of optimisation.

4.4 Adversarial Losses

In a “vanilla” GAN, an adversarial loss is a cost function that ensures that the network’s generator G produces realistic examples by comparing it against a discriminator D that distinguishes between real and fake data. These two networks play a minimax

game, trying to find a solution for the optimisation problem $\min_G \max_D \mathcal{L}_{\text{adv}}(D, G)$ [125], where adversarial loss $\mathcal{L}_{\text{adv}}(D, G)$ is defined as follows:

$$\mathcal{L}_{\text{adv}}(D, G) = \underbrace{\mathbb{E}_{x \sim p_{\text{data}}} [\log D(x)]}_{\text{real term}} + \underbrace{\mathbb{E}_{z \sim p_z} [\log(1 - D(G(z)))]}_{\text{fake term}}. \quad (5)$$

When paired data is unavailable, adversarial loss alone doesn't guarantee an invertible mapping from one domain to another since there are infinite ways to map output. Therefore, additional loss terms are introduced. CycleGAN [82], a classic architecture for unpaired domain translation (from domain A to domain B), employs two generators $G_{A \rightarrow B}$, $G_{B \rightarrow A}$ and two discriminators D_A and D_B . *Identity loss* and *cycle-consistency loss* ensure content preservation and meaningful translation between input and output (see Fig. 8b):

$$\begin{aligned} \mathcal{L}_{\text{cyc}}(G_{A \rightarrow B}, G_{B \rightarrow A}) &= \mathbb{E}_{A_{\text{real}} \sim p_{\text{data}}(A)} [\|G_{B \rightarrow A}(G_{A \rightarrow B}(A_{\text{real}})) - A_{\text{real}}\|_1] + \\ &\quad + \mathbb{E}_{B_{\text{real}} \sim p_{\text{data}}(B)} [\|G_{A \rightarrow B}(G_{B \rightarrow A}(B_{\text{real}})) - B_{\text{real}}\|_1] \\ \mathcal{L}_{\text{identity}}(G_{A \rightarrow B}, G_{B \rightarrow A}) &= \mathbb{E}_{B_{\text{real}} \sim p_{\text{data}}(B)} [\|G_{A \rightarrow B}(B_{\text{real}}) - B_{\text{real}}\|_1] + \\ &\quad + \mathbb{E}_{A_{\text{real}} \sim p_{\text{data}}(A)} [\|G_{B \rightarrow A}(A_{\text{real}}) - A_{\text{real}}\|_1] \end{aligned} \quad (6)$$

Adversarial losses aim to push low quality videos onto the manifold of high quality ones. This helps with sharper textures and richer colours than pixelwise losses alone, but it can also make training unstable and make the network to trade data fidelity for style and occasionally hallucinate details.

5 Synthetic Distorted Data Methods

As noted earlier, unsupervised learning has gained significant attention in video restoration and enhancement tasks due to the scarcity of ground truth data. An alternative approach involves the use of synthetic datasets to enable supervised training. While unsupervised methods do not require ground truth for model learning, objective evaluation, particularly with widely used metrics such as PSNR, SSIM and LPIPS, still relies on paired ground truth data. This emphasises the continued importance of synthetic datasets.

5.1 Synthetic Blur

A prevalent technique for synthesising motion blur in video datasets involves temporal averaging of frames from high frame rate sequences to simulate the effect of a long camera shutter speed. This approach was effectively utilised by Su et al. [17] in the creation of DVD dataset and by Nah et al. [126] for GOPRO dataset. To address the challenges posed by complex, non-linear motion trajectories, the NTIRE 2019 challenge on video deblurring and super-resolution introduced the REDS dataset [127]. This dataset, comprising 300 video clips of 720×1280 resolution, each with 100 frames, advanced the synthesis methodology by employing Convolutional Neural Network (CNN) based frame interpolation. By first upsampling the high frame rate source

videos, this technique increases the virtual frame rate, which helps to mitigate unnatural discontinuities or spikes in the subsequent blur trajectory. This process yields a more faithful simulation of motion blur arising from non-linear movements.

Low exposure times causing blur are common in low-light environment. Video captured in low-light conditions often suffer from high noise and low intensity as well as blur in saturated regions. LOL-Blur dataset [128] addresses this distortions and comprises 200 videos each 60 frames long for joint low-light enhancement and deblurring. The data synthesis pipeline involves simulating low-light effect with an exposure-conditional variant of Zero-DCE [129] followed generating blur via frame averaging similarly to previous methods with clipping reverse to produce realistic blur degradation in saturated areas, and finally applying generalised Gaussian filters to imitate defocus blur and adding noise generated by CycleISP [130].

To simulate a realistic depth-of-field effect for video sequences, DaBiT [19] introduces a focal blur simulator. The method begins by acquiring per-frame depth maps using the DepthAnything model [131]. A spatially-variant Gaussian blur is then applied, modulated by this depth information. The blur intensity, determined by the kernel size, is scaled symmetrically along the depth axis relative to a specified focal plane. The kernel size is zero for pixels within the focal range and increases to a pre-defined maximum for regions at the furthest depths from the focal point. This process ensures that elements progressively distant from the focal plane are rendered with an increasing level of blur, faithfully replicating a realistic focal blur effect.

5.2 Synthetic Noise

While numerous pipelines exist for synthesising realistic camera sensor noise in static images, dedicated video noise synthesis frameworks remain largely unexplored. The predominant focus of existing methods has been on modeling noise in RAW image data, with comparatively fewer approaches addressing noise characteristics specific to the sRGB color space. In the domain of RAW image noise synthesis, physics-informed statistical distributions are commonly employed. For instance, Li et al. [132] utilised the well-established Poisson-Gaussian model to simulate the combined effects of signal-dependent shot noise and signal-independent read noise. Further refining these physical models, Wei et al. [133] conducted an extensive calibration study across five different camera sensors. Their work proposed replacing the conventional Gaussian distribution with a Tukey-Lambda distribution to more accurately model read noise. In contrast, Zhang et al. [134] introduced a more generalised approach by modeling signal-dependent and signal-independent noise components separately. To ensure the synthesised noise distribution aligns with real-world sensor data, they proposed a novel domain alignment strategy. This strategy leverages both a pre-trained denoiser and a Fourier Transformer discriminator to refine the final combined noise map. A simple method proposed in [135] generates pseudo noise artefacts characteristic of underwater environments, commonly resembling snowflakes caused by biological debris (marine snow). The approach estimates marine snow by subtracting the median of multiple frames from a frame containing such artefacts. These extracted noise patterns are then added back to clean training data to simulate realistic underwater conditions.

For synthesising noise in the sRGB domain, learning-based approaches have been developed to model the complex post-processing effects inherent to this color space. Kousha et al. [136] introduced a method using normalising flows, specifically with proposed conditional linear flows. This technique conditions the network on camera metadata, such as ISO and gain settings, enabling it to learn and reproduce the distinct noise characteristics associated with different camera configurations. In contrast, Fu et al. [137] developed a camera-specific model that eliminates the need for explicit metadata. Their pipeline incorporates a gain estimation network and leverages both local and global image information to effectively model spatially-correlated noise patterns.

More recently, Zheng et al. [138] proposed a semi-supervised method based on a variational autoencoder (VAE). Their model, SenMVAE, utilises separate latent variables, \mathbf{z} and \mathbf{z}_n to disentangle image content from degradation information within the latent space, and used to construct the clean input \mathbf{x} and noisy output \mathbf{y} . A key component of their framework is a degradation level prediction network, which allows the generation process to be conditioned on a desired noise intensity, enabling controllable and varied degradation levels.

Despite the plethora of synthetic noise pipelines for images, there are significantly fewer for videos. Addressing this gap, Monakhova et al. [139] introduced a GAN-based pipeline to synthesise noisy image bursts from single, clean source images. Their generator architecture uniquely incorporates learnable parameters to sample noise from physics-informed distributions, which is then processed by a U-Net to model more complex and spatially varying noise characteristics. Lin et al. [140] approached the task in an unsupervised approach for general-use; by designing a network which estimates the noise parameters to accurately simulate the noise present in the video by randomly selecting the parameters and generating noisy inputs, and training their network to predict the input parameters.

5.3 Synthetic Low Light

Synthesising low-light content aims to reduce the illumination of the input image/video to simulate the lack of photons in the scene. Naive solutions involve applying linear and gamma transformations: $y = \alpha x^\gamma + \beta$ (or variants) [140–142] to modify the range of values from the input. However, this results in unrealistic low-light outputs. Yang et al. [143] released a synthetic low-light dataset by gathering normal-light and low-light images from multiple datasets, converting them into YCrCb color space, and applying histogram matching in the Y channel to the normal-light images.

Deep-learning methods have gained popularity as they allow for spatially-varying illumination, which is difficult for traditional methods that do not use contextual information. Triatafyllidou et al. [144] employed two CycleGANs [82] to map videos (domain A) to short-exposure still images (domain C) via an intermediate long-exposure stills domain (domain B). The network that maps domain A to domain B uses unpaired data, while the network that maps domain B to domain C uses paired long/short-exposure images from the DRV dataset [145]. Inspired by the low-light enhancement method Zero-DCE [129], Zhou et al. [128] developed a synthetic low-light

network, EC-Zero-DCE, which maps videos from normal-light to low-light by implementing a reversed curve adjustment. This network is conditioned by a parameter to control the illumination level of the output.

5.4 Synthetic Light Attenuation

Both haze and underwater image models are similarly defined as shown in Eq. 2. In hazy environments, the transmission map $t(x)$ is modeled as an exponential decay, $e^{-kd(x)}$, where $d(x)$ denotes the scene depth and k is the atmospheric scattering coefficient. A widely used synthetic dataset, HazeRD [146], simulates hazy effects based on Eq. 2, incorporating the inverse of the color transformation into the channel sensitivities to model spectral absorption. More recent approaches leverage conditional diffusion models. For example, HazeGen [147] integrates physical scattering priors and is trained on synthetic data to generate more realistic haze-like images. Xu et al. [148] generate hazy video data by applying atmospheric scattering model (Eq. 1) to videos from pre-existing datasets for downstream computer vision tasks: scene understanding [149], depth estimation [150], detection and tracking [151, 152], segmentation [153], deblurring and super-resolution [127]. To ensure temporal consistency, robust video depth estimation is used. This results in a large-scale synthetic dataset with over 5000 outdoor video sequences for various scenarios. Zhang et al. [154] introduced a hazy video dataset captured using a haze machine and repeatable camera motion facilitated by a robotic arm. These sequences, however, are limited to indoor environments.

For underwater imagery, $t(x)$ is dependent to wavelength λ as well, $t_\lambda(x) = 10^{-\beta_\lambda d(x)}$, where β_λ is the wavelength-depended medium attenuation coefficient. Scattering in the water medium is typically approximated using the Jaffe-McGlamery model [28, 29], and attenuation coefficients are adjusted to reflect different water types [155]. For learning-based approaches, Du et al. [156] generated a synthetic underwater video dataset using the pretrained Underwater Neural Rendering (UWNR) model [157], where depth maps are combined with a fixed light field map. The model is trained on the real UIEB dataset [158]. To ensure temporal consistency, all frames within a sequence share the same light field, derived from a single real underwater image.

5.5 Synthetic Atmospheric Turbulence

A common synthetic approach for simulating turbulence distortions applies predefined point spread functions (PSFs), akin to blurring. Hirsch et al. [159] introduced spatially varying degradation by applying PSFs to image patches. Chak et al. [160] extended this by randomly generating motion maps to warp clean images, followed by Gaussian blur. However, many simulation methods model atmospheric turbulence in the phase domain because a medium that is turbulent induces fluctuations in phase. For instance, Woods et al. [161] leveraged wavefront sensing principles, and Hardie et al. [162] employed a modified Von Kármán spectrum model to better represent phase distortion. Learning-based simulators have also emerged, including CNN-based models [163] and GAN-driven approaches [164]. However, as reported in the recent review by Hill et al. [20], the simulator proposed in [165] achieves superior results. This model uses Zernike polynomials to simulate phase distortions as a function of focal length,

frequency, aperture, and a random vector, introducing random tilt to the PSF. While effective for weak turbulence, their simulations tend to overestimate blur and spatial correlation under stronger conditions.

There have been efforts to replicate turbulent conditions using real heat sources. For example, gas hobs were employed in [166], with varying numbers of hobs generating different levels of distortion. Similarly, multiple heat chambers were used in [167] to produce indoor turbulence sequences. However, these real-heat approaches still oversimplify the complexity of atmospheric turbulence. A primary limitation lies in the short propagation distance of light rays through the heated medium, which does not adequately reflect the characteristics of real outdoor turbulence. Moreover, critical environmental factors, such as humidity fluctuations and airborne particles like dust, are not considered. Additionally, the resulting datasets are limited to static scenes, lacking temporal and spatial diversity present in dynamic real-world scenarios.

6 Challenges and Open Problems

Unsupervised video enhancement, despite recent significant progress, faces persistent challenges. Maintaining temporal consistency is a primary one, especially in the situations with complex or rapid motion, occlusion or abrupt scene change. Without clean reference frames to guide them, unsupervised methods can get motion wrong, causing visual problems. For example, if the camera moves quickly, the method might mistakenly add details from a moving foreground object into the background after it has left the frame. This can lead to ghosting, faint traces of the object still showing, or warping, where the background looks oddly stretched or distorted.

Another issue is handling multiple varying degradations, e.g., low light often comes with noise or loss of contrast in dark areas. In particular, for User-Generated Content (UGC) videos, which are captured by non-professionals, they are likely to suffer from low quality. Most issues are from shaky cameras, poor lighting, and compression artifacts [168]. Unsupervised enhancement methods are suited for dealing with one specific degradation type. There are some attempts to restore multiple degradation types in images, e.g., Zhang et al. [169] solve blurry and noisy images simultaneously, and Poirier-Ginter et al. [170] use unpaired learning to remove blur, noise, and artifacts. However, a general blind method that can identify and address multiple and complex combined degradation in the videos, remains an unsolved problem. Moreover, real-world videos captured in challenging conditions often suffer from a mix of distortions, where the severity of each type can vary. This makes it difficult for unified approaches to remain robust, particularly when applied to extreme degradation scenarios.

Although unsupervised models are most often trained on real world data, there is always a risk that they can overfit their training data. Additionally, the lack of groundtruth complicates robust evaluation of unsupervised approaches. One of the alternatives to evaluation on paired data is using no-reference video quality metrics. Current no-reference metrics may be biased towards certain types of degradations, have insufficient correlation with human perception or be sensitive to adversarial attacks [171]. Having said that, there aren't many no-reference metrics specifically for

video quality available. For instance, Video-BLIINDS [172] addresses this by leveraging a natural scene statistics (NSS) model of video Discrete Cosine Transform (DCT) coefficients alongside a temporal model of motion coherency.

The current approach assesses the quality of each frame (then average it), and the quality of temporal consistency separately [173]. The well-known no-reference metrics for images are NIQE (Naturalness image quality evaluator) [174], BRISQUE (Blind/Referenceless image spatial quality evaluator) [175], PIQE (Perception-based image quality evaluator) [176], and recently the learning-based method, CLIP-IQA [177]. For temporal quality, the simplest approach is to measure temporal stability by warping the previous frame to the current one and computing the mean squared error in non-occluded areas.

Finally, applicability in real-time scenarios is crucial for many practical video applications, especially in downstream machine vision tasks such as object detection, recognition, and tracking. This is particularly critical in domains like autonomous driving, where decisions must be made instantaneously, or in medical imaging, where enhanced real-time feedback can support diagnosis or intervention. In such settings, video restoration and enhancement methods must not only produce high-quality outputs but also operate with minimal latency to ensure timely and reliable responses. However, achieving this balance between visual quality and computational efficiency remains a significant challenge. Therefore, the development of lightweight, efficient, and robust unsupervised models capable of handling diverse degradation types while meeting real-time constraints is a pressing need. Future research should explore strategies such as model distillation, adaptive inference, or spatiotemporal redundancy exploitation to bridge this gap between quality and speed.

7 Conclusion

This survey traces the progression of video restoration and enhancement techniques, starting from traditional methods based on physical models and handcrafted priors, through the rise of supervised deep learning methods that rely on paired training data, to the contemporary unsupervised, self-supervised and zero-shot strategies that offer solutions for video degradations in conditions with no access to ground truth. We synthesised recent approaches and architectural design principles in unsupervised video denoising, deblurring, dehazing, and low-light enhancement, highlighting several key directions: domain translation, self-supervised signal design, consistency-based methods, degradation-aware approaches and methods relying on explicit or learned implicit priors. We also looked into types of objective functions used for video enhancement, including losses for reference fidelity, data-consistency losses, prior-based losses and losses used in adversarial methods.

Finally, we addressed the role of synthetic datasets in supporting both supervised training and objective evaluation of unsupervised video enhancement approaches. While unsupervised methods do not rely on ground-truth data during training stage, metrics such as PSNR, SSIM, and LPIPS still require paired references. Synthetic distortions, such as blur, noise, low-light conditions, light attenuation, and atmospheric

turbulence, provide controlled settings for training and benchmarking, and thus remain essential the progress in video restoration.

References

- [1] Yao, R., Lin, G., Xia, S., Zhao, J., Zhou, Y.: Video object segmentation and tracking: A survey. *ACM Trans. Intell. Syst. Technol.* **11**(4) (2020) <https://doi.org/10.1145/3391743>
- [2] Yi, A., Anantrasirichai, N.: A comprehensive study of object tracking in low-light environments. *Sensors* **24**(14) (2024)
- [3] Hill, P., Achim, A., Bull, D., Anantrasirichai, N.: Automatic object detection in atmospheric turbulence-affected environments. In: *Proceedings of SPIE – Automatic Target Recognition XXXV*, vol. 13463, pp. 145–147 (2025). <https://doi.org/10.1117/12.3053981>
- [4] Aja-Fernández, S., Curiale, A.H., Prince, J.L.: Chapter 6 - image filtering: enhancement and restoration. In: Frangi, A.F., Prince, J.L., Sonka, M. (eds.) *Medical Image Analysis. The MICCAI Society book Series*, pp. 145–176. Academic Press, ??? (2024). <https://doi.org/10.1016/B978-0-12-813657-7.00019-4>
- [5] Anantrasirichai, N., Bull, D.: Artificial intelligence in the creative industries: a review. *Artificial Intelligence Review* **55**, 589–656 (2022) <https://doi.org/10.1007/s10462-021-10039-7>
- [6] Celebi, M.E., Lecca, M., Smolka, B. (eds.): *Color Image and Video Enhancement*. Springer, ??? (2015). <https://doi.org/10.1007/978-3-319-09363-5>
- [7] Yu, G., Sapiro, G.: Image enhancement and restoration: Traditional approaches. In: *Computer Vision* (2020). https://doi.org/10.1007/978-3-030-03243-2_233-1 . https://doi.org/10.1007/978-3-030-03243-2_233-1
- [8] Anantrasirichai, N., Zhang, F., Bull, D.: Artificial intelligence in creative industries: Advances prior to 2025. *arXiv preprint arXiv:2501.02725* (2025)
- [9] Zhang, F., Li, Y., You, S., Fu, Y.: Learning temporal consistency for low light video enhancement from single images. In: *2021 IEEE/CVF Conference on Computer Vision and Pattern Recognition (CVPR)*, pp. 4965–4974 (2021). <https://doi.org/10.1109/CVPR46437.2021.00493>
- [10] Cao, C., Yue, H., Liu, X., Yang, J.: Zero-shot video restoration and enhancement using pre-trained image diffusion model. In: *Proceedings of the AAAI Conference on Artificial Intelligence*, vol. 39, pp. 1935–1943 (2025). <https://doi.org/10.1609/aaai.v39i2.32189> . <https://doi.org/10.1609/aaai.v39i2.32189>
- [11] Huang, T., Li, S., Jia, X., Lu, H., Liu, J.: Neighbor2neighbor: Self-supervised

- denoising from single noisy images. In: Proceedings of the IEEE/CVF Conference on Computer Vision and Pattern Recognition (CVPR), pp. 14781–14790 (2021)
- [12] Liu, R., Zhu, Y., Luo, G.B.: Appearance consistency and motion coherence learning for internal video inpainting. *CAAI Transactions on Intelligence Technology*, 1–15 (2025) <https://doi.org/10.1049/cit2.12405>
 - [13] Wang, J., Jiao, J., Bao, L., He, S., Liu, Y., Liu, W.: Self-supervised spatio-temporal representation learning for videos by predicting motion and appearance statistics. In: Proceedings of the IEEE/CVF Conference on Computer Vision and Pattern Recognition (CVPR) (2019)
 - [14] Rota, C., Buzzelli, M., Bianco, S., Schettini, R.: Video restoration based on deep learning: A comprehensive survey. *Artificial Intelligence Review* **56**, 5317–5364 (2023) <https://doi.org/10.1007/s10462-022-10302-5>
 - [15] Li, C., Guo, C., Han, L., Jiang, J., Cheng, M.-M., Gu, J., Loy, C.C.: Low-light image and video enhancement using deep learning: A survey. *IEEE Transactions on Pattern Analysis and Machine Intelligence* **44**(12), 9396–9416 (2022) <https://doi.org/10.1109/TPAMI.2021.3126387>
 - [16] Hu, K., Weng, C., Zhang, Y., Jin, J., Xia, Q.: An overview of underwater vision enhancement: From traditional methods to recent deep learning. *Journal of Marine Science and Engineering* **10**(2), 241 (2022) <https://doi.org/10.3390/jmse10020241>
 - [17] Su, S., Delbracio, M., Wang, J., Sapiro, G., Heidrich, W., Wang, O.: Deep video deblurring for hand-held cameras. In: Proceedings of the IEEE Conference on Computer Vision and Pattern Recognition, pp. 1279–1288 (2017)
 - [18] Xiang, Y., Zhou, H., Li, C., *et al.*: Deep learning in motion deblurring: Current status, benchmarks and future prospects. *The Visual Computer* **41**, 3801–3827 (2025) <https://doi.org/10.1007/s00371-024-03632-8>
 - [19] Morris, C., Anantrasirichai, N., Zhang, F., Bull, D.: DaBiT: Depth and blur informed transformer for video focal deblurring. In: 2025 IEEE/CVF Winter Conference on Applications of Computer Vision Workshops (WACVW), pp. 278–288 (2025). <https://doi.org/10.1109/WACVW65960.2025.00038>
 - [20] Hill, P., Anantrasirichai, N., Achim, A., Bull, D.: Deep learning techniques for atmospheric turbulence removal: A review. *Artificial Intelligence Review* **58**, 101 (2025) <https://doi.org/10.1007/s10462-024-11086-6>
 - [21] Richards, J.A.: Remote Sensing Digital Image Analysis. Springer, ??? (2022). <https://doi.org/10.1007/978-3-030-82327-6> . <https://doi.org/10.1007/978-3-030-82327-6>

- [22] Nah, S., Kim, T.H., Lee, K.M.: Deep multi-scale convolutional neural network for dynamic scene deblurring. In: CVPR (2017)
- [23] Blanksby, A.J., Loinaz, M.J., Inglis, D., Ackland, B.D.: Noise performance of a color cmos photogate image sensor. In: International Electron Devices Meeting. IEDM Technical Digest, pp. 205–208 (1997). IEEE
- [24] Foi, A., Trimeche, M., Katkovnik, V., Egiazarian, K.: Practical poissonian-gaussian noise modeling and fitting for single-image raw-data. IEEE transactions on image processing **17**(10), 1737–1754 (2008)
- [25] Malyugina, A., Anantrasirichai, N., Bull, D.: A topological loss function for image denoising on a new BVI-lowlight dataset. Signal Processing **211**, 109081 (2024) <https://doi.org/10.1016/j.sigpro.2024.109081>
- [26] Nayar, S.K., Narasimhan, S.G.: Vision in bad weather. In: Proceedings of the IEEE International Conference on Computer Vision (ICCV), vol. 2, pp. 820–827 (1999). <https://doi.org/10.1109/ICCV.1999.790306>
- [27] Goyal, B., Dogra, A., Lepcha, D.C., Goyal, V., Alkhayyat, A., Chohan, J.S., Kukreja, V.: Recent advances in image dehazing: Formal analysis to automated approaches. Information Fusion **104**, 102151 (2024) <https://doi.org/10.1016/j.inffus.2023.102151>
- [28] Jaffe, J.S.: Computer modeling and the design of optimal underwater imaging systems. IEEE Journal of Oceanic Engineering **15**(2), 101–111 (1990)
- [29] McGlamery, B.L.: A computer model for underwater camera systems. In: Ocean Optics VI (1980)
- [30] Kim, J.-H., Jang, W.-D., Sim, J.-Y., Kim, C.-S.: Optimized contrast enhancement for real-time image and video dehazing. Journal of Visual Communication and Image Representation **24**(3), 410–425 (2013)
- [31] Ren, W., Tian, J., Han, Z., Chan, A., Tang, Y.: Video desnowing and deraining based on matrix decomposition. In: Proceedings of the IEEE Conference on Computer Vision and Pattern Recognition, pp. 4210–4219 (2017)
- [32] Anantrasirichai, N., Malyugina, A., Lin, R., Bull, D.: BVI-Lowlight: Fully Registered Datasets for Low-light Image and Video Enhancement. <https://doi.org/10.21227/mzny-8c77> . <https://dx.doi.org/10.21227/mzny-8c77>
- [33] Chan, S.H., Wang, X., Elgendy, O.A.: Plug-and-play admm for image restoration: Fixed-point convergence and applications. IEEE Transactions on Computational Imaging **3**(1), 84–98 (2017) <https://doi.org/10.1109/TCI.2016.2629286>
- [34] Lee, J.-S.: Digital image enhancement and noise filtering by use of local statistics.

- IEEE transactions on pattern analysis and machine intelligence (2), 165–168 (1980)
- [35] Ghazal, M., Amer, A., Ghrayeb, A.: Structure-oriented multidirectional wiener filter for denoising of image and video signals. *IEEE Transactions on circuits and systems for video technology* **18**(12), 1797–1802 (2008)
 - [36] Dubois, E., Sabri, S.: Noise reduction in image sequences using motion-compensated temporal filtering. *IEEE transactions on communications* **32**(7), 826–831 (2003)
 - [37] Hsia, S.-C., Hsu, W.-C., Tsai, C.-L.: High-efficiency tv video noise reduction through adaptive spatial–temporal frame filtering. *Journal of Real-Time Image Processing* **10**, 561–572 (2015)
 - [38] Yahya, A., Tan, J., Li, L.: Video noise reduction method using adaptive spatial-temporal filtering. *Discrete Dynamics in Nature and Society* **2015**, 1–10 (2015) <https://doi.org/10.1155/2015/351763>
 - [39] Dabov, K., Foi, A., Katkovnik, V., Egiazarian, K.: Image denoising by sparse 3-d transform-domain collaborative filtering. *IEEE Transactions on image processing* **16**(8), 2080–2095 (2007)
 - [40] Dabov, K., Foi, A., Egiazarian, K.: Video denoising by sparse 3d transform-domain collaborative filtering. In: 2007 15th European Signal Processing Conference, pp. 145–149 (2007)
 - [41] Li, Z., Dong, Z., Yu, A., He, Z., Yi, T.: An enhanced v-bm3d algorithm for videosar denoising combined with temporal information. In: 2019 IEEE 4th International Conference on Signal and Image Processing (ICSIP), pp. 994–998 (2019). IEEE
 - [42] Maggioni, M., Boracchi, G., Foi, A., Egiazarian, K.: Video denoising, deblocking, and enhancement through separable 4-d nonlocal spatiotemporal transforms. *IEEE Transactions on image processing* **21**(9), 3952–3966 (2012)
 - [43] Zhang, J., Li, L., Zhang, Y., Yang, G., Cao, X., Sun, J.: Video dehazing with spatial and temporal coherence. *The Visual Computer* **27**, 749–757 (2011)
 - [44] He, K., Sun, J., Tang, X.: Single image haze removal using dark channel prior. *IEEE transactions on pattern analysis and machine intelligence* **33**(12), 2341–2353 (2010)
 - [45] Lin, Z., Wang, X.: Dehazing for image and video using guided filter. *Open Journal of Applied Sciences* **2**(4), 123–127 (2013)

- [46] Song, Y., Luo, H., Hui, B., Chang, Z.: An improved image dehazing and enhancing method using dark channel prior. In: The 27th Chinese Control and Decision Conference (2015 CCDC), pp. 5840–5845 (2015). IEEE
- [47] Lee, S., Yun, S., Nam, J.-H., Won, C.S., Jung, S.-W.: A review on dark channel prior based image dehazing algorithms. *EURASIP Journal on Image and Video Processing* **2016**, 1–23 (2016)
- [48] Lv, X., Chen, W., Shen, I.-f.: Real-time dehazing for image and video. In: 2010 18th Pacific Conference on Computer Graphics and Applications, pp. 62–69 (2010). <https://doi.org/10.1109/PacificGraphics.2010.16>
- [49] Adidela, S., Singh, S., Sahu, T., Mishra, A.: Single image and video dehazing: A dark channel prior (dcp)-based approach. In: 2021 IEEE 18th India Council International Conference (INDICON), pp. 1–6 (2021). IEEE
- [50] Park, Y., Kim, T.-H.: Fast execution schemes for dark-channel-prior-based outdoor video dehazing. *IEEE Access* **6**, 10003–10014 (2018)
- [51] Biswas, P., Sarkar, A.S., Mynuddin, M.: Deblurring images using a wiener filter. *International Journal of Computer Applications* **109**(7), 36–38 (2015)
- [52] Richardson, W.H.: Bayesian-based iterative method of image restoration. *Journal of the optical society of America* **62**(1), 55–59 (1972)
- [53] Cai, J.-F., Ji, H., Liu, C., Shen, Z.: Blind motion deblurring using multiple images. *Journal of computational physics* **228**(14), 5057–5071 (2009)
- [54] Aubailly, M., Vorontsov, M.A., Carhart, G.W., Valley, M.T.: Automated video enhancement from a stream of atmospherically-distorted images: the lucky-region fusion approach. In: *Atmospheric Optics: Models, Measurements, and Target-in-the-Loop Propagation III*, vol. 7463, pp. 104–113 (2009). SPIE
- [55] Lou, Y., Kang, S.H., Soatto, S., Bertozzi, A.L.: Video stabilization of atmospheric turbulence distortion. *Inverse Problems and Imaging* **7**(3), 839–861 (2013)
- [56] Zhu, X., Milanfar, P.: Stabilizing and deblurring atmospheric turbulence. In: 2011 IEEE International Conference on Computational Photography (ICCP), pp. 1–8 (2011). IEEE
- [57] Anantrasirichai, N., Achim, A., Kingsbury, N.G., Bull, D.R.: Atmospheric turbulence mitigation using complex wavelet-based fusion. *IEEE Transactions on Image Processing* **22**(6), 2398–2408 (2013)
- [58] Kim, T.K., Paik, J.K., Kang, B.S.: Contrast enhancement system using spatially adaptive histogram equalization with temporal filtering. *IEEE Transactions on*

- [59] Zuiderveld, K.J., *et al.*: Contrast limited adaptive histogram equalization. *Graphics gems* **4**(1), 474–485 (1994)
- [60] Land, E.H., McCann, J.J.: Lightness and retinex theory. *Journal of the Optical Society of America* **61**(1), 1–11 (1971) <https://doi.org/10.1364/JOSA.61.000001>
- [61] Guo, X.: Lime: A method for low-light image enhancement. In: *Proceedings of the 24th ACM International Conference on Multimedia*. MM '16, pp. 87–91. Association for Computing Machinery, New York, NY, USA (2016). <https://doi.org/10.1145/2964284.2967188> . <https://doi.org/10.1145/2964284.2967188>
- [62] Jobson, D.J., Rahman, Z.-u., Woodell, G.A.: Properties and performance of a center/surround retinex. *IEEE transactions on image processing* **6**(3), 451–462 (1997)
- [63] Jobson, D.J., Rahman, Z.-u., Woodell, G.A.: A multiscale retinex for bridging the gap between color images and the human observation of scenes. *IEEE Transactions on Image processing* **6**(7), 965–976 (1997)
- [64] Sheeba, M., Christopher, C.S.: A review on video denoising methods. In: *2019 International Conference on Recent Advances in Energy-efficient Computing and Communication (ICRAECC)*, pp. 1–6 (2019). IEEE
- [65] Reddy, S.: Advancements in video deblurring: A comprehensive review. *INTERNATIONAL JOURNAL OF SCIENTIFIC RESEARCH IN ENGINEERING AND MANAGEMENT* **08**, 1–5 (2024) <https://doi.org/10.55041/IJSREM32759>
- [66] Ayoub, A., El-Shafai, W., El-Samie, F.E.A., Hamad, E.K., EL-Rabaie, E.-S.M.: Review of dehazing techniques: Challenges and future trends. *Multimedia Tools and Applications*, 1–29 (2024)
- [67] Li, C., Guo, C., Han, L., Jiang, J., Cheng, M.-M., Gu, J., Loy, C.C.: Low-light image and video enhancement using deep learning: A survey. *IEEE transactions on pattern analysis and machine intelligence* **44**(12), 9396–9416 (2021)
- [68] Ye, J., Qiu, C., Zhang, Z.: A survey on learning-based low-light image and video enhancement. *Displays* **81**, 102614 (2024)
- [69] Zheng, S., Ma, Y., Pan, J., Lu, C., Gupta, G.: Low-light image and video enhancement: A comprehensive survey and beyond. *arXiv preprint arXiv:2212.10772* (2022)
- [70] Wang, H., Wu, Y., Li, M., Zhao, Q., Meng, D.: Survey on rain removal from videos or a single image. *Science China Information Sciences* **65**(1), 111101 (2022)

- [71] Hill, P., Anantrasirichai, N., Achim, A., Bull, D.: Deep learning techniques for atmospheric turbulence removal: a review. *Artificial Intelligence Review* **58**(4), 101 (2025)
- [72] Lhiadi, R., Jaddar, A., Kaaouachi, A.: Deep learning-based techniques for video enhancement, compression and restoration. *IAES International Journal of Artificial Intelligence (IJ-AI)* **14**, 1518 (2025) <https://doi.org/10.11591/ijai.v14.i2.pp1518-1530>
- [73] Ronneberger, O., Fischer, P., Brox, T.: U-net: Convolutional networks for biomedical image segmentation. In: *Medical Image Computing and Computer-assisted intervention—MICCAI 2015: 18th International Conference, Munich, Germany, October 5-9, 2015, Proceedings, Part III* 18, pp. 234–241 (2015). Springer
- [74] Tassano, M., Delon, J., Veit, T.: Fastdvdnet: Towards real-time deep video denoising without flow estimation. In: *Proceedings of the IEEE/CVF Conference on Computer Vision and Pattern Recognition*, pp. 1351–1360 (2020)
- [75] Yue, H., Cao, C., Liao, L., Chu, R., Yang, J.: Supervised raw video denoising with a benchmark dataset on dynamic scenes. In: *Proceedings of the IEEE/CVF Conference on Computer Vision and Pattern Recognition*, pp. 2301–2310 (2020)
- [76] Li, R., Chen, L.: Progressive deep video dehazing without explicit alignment estimation. *Applied Intelligence* **53**(10), 12437–12447 (2023)
- [77] Chan, K.C., Wang, X., Yu, K., Dong, C., Loy, C.C.: Basicvsr: The search for essential components in video super-resolution and beyond. In: *Proceedings of the IEEE/CVF Conference on Computer Vision and Pattern Recognition*, pp. 4947–4956 (2021)
- [78] Chan, K.C., Zhou, S., Xu, X., Loy, C.C.: Basicvsr++: Improving video super-resolution with enhanced propagation and alignment. In: *Proceedings of the IEEE/CVF Conference on Computer Vision and Pattern Recognition*, pp. 5970–5979 (2022)
- [79] Yang, W., Liu, J., Feng, J.: Frame-consistent recurrent video deraining with dual-level flow. In: *Proceedings of the IEEE/CVF Conference on Computer Vision and Pattern Recognition*, pp. 1661–1670 (2019)
- [80] Liang, J., Cao, J., Fan, Y., Zhang, K., Ranjan, R., Li, Y., Timofte, R., Van Gool, L.: Vrt: A video restoration transformer. In: *Proceedings of the IEEE/CVF Conference on Computer Vision and Pattern Recognition*, pp. 1450–1460 (2022)
- [81] Jing, L., Tian, Y.: Self-Supervised Visual Feature Learning With Deep Neural Networks: A Survey **43**(11), 4037–4058 <https://doi.org/10.1109/TPAMI.2020.2992393> . Accessed 2025-05-26

- [82] Zhu, J.-Y., Park, T., Isola, P., Efros, A.A.: Unpaired Image-To-Image Translation Using Cycle-Consistent Adversarial Networks, pp. 2223–2232
- [83] Anantrasirichai, N., Bull, D.: Contextual colorization and denoising for low-light ultra high resolution sequences. In: 2021 IEEE International Conference on Image Processing (ICIP), pp. 1614–1618 (2021). <https://doi.org/10.1109/ICIP42928.2021.9506694>
- [84] Fuoli, D., Huang, Z., Paudel, D.P., Van Gool, L., Timofte, R.: An Efficient Recurrent Adversarial Framework for Unsupervised Real-Time Video Enhancement **131**(4), 1042–1059 <https://doi.org/10.1007/s11263-022-01735-0> . Accessed 2025-05-26
- [85] Patil, P.W., Randive, S.N., Gupta, S., Rana, S., Venkatesh, S., Murala, S.: Unpaired recurrent learning for real-world video de-hazing **166**, 111698 <https://doi.org/10.1016/j.patcog.2025.111698> . Accessed 2025-05-26
- [86] Lv, X., Zhang, S., Wang, C., Zhang, W., Yao, H., Huang, Q.: Unsupervised Low-Light Video Enhancement With Spatial-Temporal Co-Attention Transformer **32**, 4701–4715 <https://doi.org/10.1109/TIP.2023.3301332> . Accessed 2025-05-26
- [87] Li, X., Ren, Y., Jin, X., Lan, C., Wang, X., Zeng, W., Wang, X., Chen, Z.: Diffusion models for image restoration and enhancement – a comprehensive survey. arXiv:2308.09388 (2023)
- [88] Sheth, D.Y., Mohan, S., Vincent, J.L., Manzorro, R., Crozier, P.A., Khapra, M.M., Simoncelli, E.P., Fernandez-Granda, C.: Unsupervised Deep Video Denoising. In: 2021 IEEE/CVF International Conference on Computer Vision (ICCV), pp. 1739–1748. IEEE. <https://doi.org/10.1109/ICCV48922.2021.00178> . <https://ieeexplore.ieee.org/document/9711126/> Accessed 2025-05-21
- [89] Lehtinen, J., Munkberg, J., Hasselgren, J., Laine, S., Karras, T., Aittala, M., Aila, T.: Noise2noise: Learning image restoration without clean data. arXiv preprint arXiv:1803.04189 (2018)
- [90] Dewil, V., Anger, J., Davy, A., Ehret, T., Facciolo, G., Arias, P.: Self-supervised training for blind multi-frame video denoising. In: 2021 IEEE Winter Conference on Applications of Computer Vision (WACV), pp. 2723–2733. IEEE. <https://doi.org/10.1109/WACV48630.2021.00277> . <https://ieeexplore.ieee.org/document/9423377/> Accessed 2025-05-19
- [91] Wang, Z., Zhang, Y., Zhang, D., Fu, Y.: Recurrent Self-Supervised Video Denoising with Denser Receptive Field. In: Proceedings of the 31st ACM International Conference on Multimedia, pp. 7363–7372. ACM. <https://doi.org/10.1145/3581783.3612228> . <https://dl.acm.org/doi/10.1145/3581783.3612228> Accessed 2025-05-15

- [92] Chen, Z., Jiang, T., Hu, X., Zhang, W., Li, H., Wang, H.: Spatiotemporal blind-spot network with calibrated flow alignment for self-supervised video denoising. In: Proceedings of the AAAI Conference on Artificial Intelligence, vol. 39, pp. 2411–2419 (2025). <https://doi.org/10.1609/aaai.v39i3.32242> . <https://doi.org/10.1609/aaai.v39i3.32242>
- [93] Lyu, X., Hou, J.: Enhancing low-light light field images with a deep compensation unfolding network. *IEEE Transactions on Image Processing* (2024)
- [94] Wu, W., Weng, J., Zhang, P., Wang, X., Yang, W., Jiang, J.: Uretinex-net: Retinex-based deep unfolding network for low-light image enhancement. In: Proceedings of the IEEE/CVF Conference on Computer Vision and Pattern Recognition, pp. 5901–5910 (2022)
- [95] Zhu, L., Yang, W., Chen, B., Zhu, H., Ni, Z., Mao, Q., Wang, S.: Unrolled Decomposed Unpaired Learning for Controllable Low-Light Video Enhancement. In: Leonardis, A., Ricci, E., Roth, S., Russakovsky, O., Sattler, T., Varol, G. (eds.) *Computer Vision – ECCV 2024* vol. 15081, pp. 329–347. Springer. https://doi.org/10.1007/978-3-031-73337-6_19 . https://link.springer.com/10.1007/978-3-031-73337-6_19 Accessed 2025-05-19
- [96] Wang, R., Xu, X., Fu, C.-W., Lu, J., Yu, B., Jia, J.: Seeing dynamic scene in the dark: A high-quality video dataset with mechatronic alignment. In: Proceedings of the IEEE/CVF International Conference on Computer Vision, pp. 9700–9709 (2021)
- [97] Ryu, E., Liu, J., Wang, S., Chen, X., Wang, Z., Yin, W.: Plug-and-play methods provably converge with properly trained denoisers. In: Proceedings of the 36th International Conference on Machine Learning (ICML), pp. 5546–5557 (2019)
- [98] Nair, P., Chaudhury, K.N.: Plug-and-play regularization using linear solvers. *IEEE Transactions on Image Processing* **31**, 6344–6355 (2022) <https://doi.org/10.1109/TIP.2022.3211473>
- [99] Zhang, K., Li, Y., Zuo, W., Zhang, L., Van Gool, L., Timofte, R.: Plug-and-play image restoration with deep denoiser prior. *IEEE Transactions on Pattern Analysis and Machine Intelligence* **44**(10), 6360–6376 (2022) <https://doi.org/10.1109/TPAMI.2021.3088914>
- [100] Kamilov, U.S., Bouman, C.A., Buzzard, G.T., Wohlberg, B.: Plug-and-play methods for integrating physical and learned models in computational imaging: Theory, algorithms, and applications. *IEEE Signal Processing Magazine* **40**(1), 85–97 (2023) <https://doi.org/10.1109/MSP.2022.3199595>
- [101] Yuan, X., Liu, Y., Suo, J., Durand, F., Dai, Q.: Plug-and-play algorithms for video snapshot compressive imaging. *IEEE Transactions on Pattern Analysis and Machine Intelligence* **44**(10), 7093–7111 (2022) <https://doi.org/10.1109/>

- [102] Tassano, M., Delon, J., Veit, T.: Fastdvdnet: Towards real-time deep video denoising without flow estimation. In: 2020 IEEE/CVF Conference on Computer Vision and Pattern Recognition (CVPR), pp. 1351–1360 (2020). <https://doi.org/10.1109/CVPR42600.2020.00143>
- [103] Zerva, M.C., Kondi, L.P.: Video super-resolution using plug-and-play priors. *IEEE Access* **12**, 11963–11971 (2024) <https://doi.org/10.1109/ACCESS.2024.3355195>
- [104] Zhang, K., Zuo, W., Chen, Y., Meng, D., Zhang, L.: Beyond a gaussian denoiser: Residual learning of deep cnn for image denoising. *IEEE Transactions on Image Processing* **26**(7), 3142–3155 (2017) <https://doi.org/10.1109/TIP.2017.2662206>
- [105] Lin, J., Hu, X., Cai, Y., Wang, H., Yan, Y., Zou, X., Zhang, Y., Gool, L.V.: Unsupervised Flow-Aligned Sequence-to-Sequence Learning for Video Restoration
- [106] Yeh, C.-H., Lin, C.-Y., Wang, Z., Hsiao, C.-W., Chen, T.-H., Shiu, H.-S., Liu, Y.-L.: DiffIR2VR-Zero: Zero-Shot Video Restoration with Diffusion-based Image Restoration Models. <https://doi.org/10.48550/arXiv.2407.01519> . <http://arxiv.org/abs/2407.01519> Accessed 2025-05-26
- [107] Varghese, N., Kumar, A., Rajagopalan, A.N.: Self-supervised monocular underwater depth recovery, image restoration, and a real-sea video dataset. In: *Proceedings of the IEEE/CVF International Conference on Computer Vision (ICCV)*, pp. 12248–12258 (2023)
- [108] Fu, Z., Guo, L., Wang, C., Wang, Y., Li, Z., Wen, B.: Temporal As a Plugin: Unsupervised Video Denoising with Pre-trained Image Denoisers. In: *Computer Vision – ECCV 2024: 18th European Conference, Milan, Italy, September 29–October 4, 2024, Proceedings, Part LVI*, pp. 349–367. Springer. https://doi.org/10.1007/978-3-031-72992-8_20 . https://doi.org/10.1007/978-3-031-72992-8_20 Accessed 2025-05-21
- [109] Zheng, S., Gupta, G.: Semantic-Guided Zero-Shot Learning for Low-Light Image/Video Enhancement. In: 2022 IEEE/CVF Winter Conference on Applications of Computer Vision Workshops (WACVW), pp. 581–590. IEEE. <https://doi.org/10.1109/WACVW54805.2022.00064> . <https://ieeexplore.ieee.org/document/9707578/> Accessed 2025-05-15
- [110] Chen, H., Gu, J., Gallo, O., Liu, M.-Y., Veeraraghavan, A., Kautz, J.: Reblur2Deblur: Deblurring videos via self-supervised learning. In: 2018 IEEE International Conference on Computational Photography (ICCP), pp. 1–9. <https://doi.org/10.1109/ICCPHOT.2018.8368468> . <https://ieeexplore.ieee.org/document/8368468/> Accessed 2025-05-15

- [111] Lee, S., Cho, D., Kim, J., Kim, T.H.: Restore from Restored: Video Restoration with Pseudo Clean Video. In: 2021 IEEE/CVF Conference on Computer Vision and Pattern Recognition (CVPR), pp. 3536–3545. IEEE. <https://doi.org/10.1109/CVPR46437.2021.00354> . <https://ieeexplore.ieee.org/document/9578402/> Accessed 2025-05-19
- [112] Ehret, T., Davy, A., Morel, J.-M., Facciolo, G., Arias, P.: Model-blind video denoising via frame-to-frame training. In: Proceedings of the IEEE/CVF Conference on Computer Vision and Pattern Recognition, pp. 11369–11378 (2019)
- [113] Zheng, H., Pang, T., Ji, H.: Unsupervised Deep Video Denoising with Untrained Network **37**(3), 3651–3659 <https://doi.org/10.1609/aaai.v37i3.25476> . Accessed 2025-05-26
- [114] Li, Y., Anantrasirichai, N.: Zero-TIG: Temporal consistency-aware zero-shot illumination-guided low-light video enhancement. In: European Signal Processing Conference (2025)
- [115] Shi, Y., Liu, D., Zhang, L., Tian, Y., Xia, X., Fu, X.: Zero-ig: zero-shot illumination-guided joint denoising and adaptive enhancement for low-light images. In: Proceedings of the IEEE/CVF Conference on Computer Vision and Pattern Recognition, pp. 3015–3024 (2024)
- [116] Pandey, P., Gupta, R., Goel, N.: Comprehensive review of single image defogging techniques: enhancement, prior, and learning based approaches. Artificial Intelligence Review **58**(116) (2025) <https://doi.org/10.1007/s10462-024-11034-4>
- [117] Ulyanov, D., Vedaldi, A., Lempitsky, V.: Deep image prior. In: Proceedings of the IEEE Conference on Computer Vision and Pattern Recognition, pp. 9446–9454 (2018)
- [118] Pan, X., Zhan, X., Dai, B., Lin, D., Loy, C.C., Luo, P.: Exploiting deep generative prior for versatile image restoration and manipulation. IEEE Transactions on Pattern Analysis and Machine Intelligence **44**(11), 7474–7489 (2022) <https://doi.org/10.1109/TPAMI.2021.3115428>
- [119] Kavar, B., Elad, M., Ermon, S., Song, J.: Denoising diffusion restoration models. In: Koyejo, S., Mohamed, S., Agarwal, A., Belgrave, D., Cho, K., Oh, A. (eds.) Advances in Neural Information Processing Systems, vol. 35, pp. 23593–23606. Curran Associates, Inc., ??? (2022). https://proceedings.neurips.cc/paper_files/paper/2022/file/95504595b6169131b6ed6cd72eb05616-Paper-Conference.pdf
- [120] Srinath, S., Chandrasekar, A., Jamadagni, H., Soundararajan, R., A P, P.: UnDIVE: Generalized underwater video enhancement using generative priors. In: 2025 IEEE/CVF Winter Conference on Applications of Computer Vision (WACV), pp. 9001–9012 (2025). <https://doi.org/10.1109/WACV61041.2025.00872>

- [121] Ho, J., Jain, A., Abbeel, P.: Denoising diffusion probabilistic models. In: Advances in Neural Information Processing Systems (NeurIPS), vol. 33, pp. 6840–6851 (2020)
- [122] Wen, Y., Gao, T., Chen, T.: Unpaired photo-realistic image deraining with energy-informed diffusion model. In: Proceedings of the 32nd ACM International Conference on Multimedia. MM '24, pp. 360–369 (2024). <https://doi.org/10.1145/3664647.3680560>
- [123] Radford, A., Kim, J.W., Hallacy, C., Ramesh, A., Goh, G., Agarwal, S., Sasstry, S., Askell, A., Mishkin, P., Clark, J., Krueger, G., Sutskever, I.: Learning transferable visual models from natural language supervision. In: Proceedings of the 38th International Conference on Machine Learning (ICML), vol. 139, pp. 8748–8763 (2021). PMLR
- [124] Shrivastava, G., Lim, S.N., Shrivastava, A.: Video dynamics prior: An internal learning approach for robust video enhancements. In: Oh, A., Naumann, T., Globerson, A., Saenko, K., Hardt, M., Levine, S. (eds.) Advances in Neural Information Processing Systems, vol. 36, pp. 34228–34246. Curran Associates, Inc., ??? (2023). https://proceedings.neurips.cc/paper_files/paper/2023/file/6ba85c6f1c7656a6a647bc4d63b90bf0-Paper-Conference.pdf
- [125] Goodfellow, I., Pouget-Abadie, J., Mirza, M., Xu, B., Warde-Farley, D., Ozair, S., Courville, A., Bengio, Y.: Generative adversarial networks. Communications of the ACM **63**(11), 139–144 (2020)
- [126] Nah, S., Hyun Kim, T., Mu Lee, K.: Deep multi-scale convolutional neural network for dynamic scene deblurring. In: Proceedings of the IEEE Conference on Computer Vision and Pattern Recognition, pp. 3883–3891 (2017)
- [127] Nah, S., Baik, S., Hong, S., Moon, G., Son, S., Timofte, R., Mu Lee, K.: Ntire 2019 challenge on video deblurring and super-resolution: Dataset and study. In: Proceedings of the IEEE/CVF Conference on Computer Vision and Pattern Recognition Workshops, pp. 0–0 (2019)
- [128] Zhou, S., Li, C., Change Loy, C.: Lednet: Joint low-light enhancement and deblurring in the dark. In: European Conference on Computer Vision, pp. 573–589 (2022). Springer
- [129] Guo, C., Li, C., Guo, J., Loy, C.C., Hou, J., Kwong, S., Cong, R.: Zero-reference deep curve estimation for low-light image enhancement. In: Proceedings of the IEEE/CVF Conference on Computer Vision and Pattern Recognition, pp. 1780–1789 (2020)
- [130] Zamir, S.W., Arora, A., Khan, S., Hayat, M., Khan, F.S., Yang, M.-H., Shao, L.: Cycleisp: Real image restoration via improved data synthesis. In: Proceedings of

- the IEEE/CVF Conference on Computer Vision and Pattern Recognition, pp. 2696–2705 (2020)
- [131] Yang, L., Kang, B., Huang, Z., Xu, X., Feng, J., Zhao, H.: Depth Anything: Unleashing the power of large-scale unlabeled data. In: 2024 IEEE/CVF Conference on Computer Vision and Pattern Recognition (CVPR), pp. 10371–10381 (2024). <https://doi.org/10.1109/CVPR52733.2024.00987>
 - [132] Li, R., Wang, Y., Chen, S., Zhang, F., Gu, J., Xue, T.: Dualdn: Dual-domain denoising via differentiable isp. In: European Conference on Computer Vision, pp. 160–177 (2025). Springer
 - [133] Wei, K., Fu, Y., Zheng, Y., Yang, J.: Physics-based noise modeling for extreme low-light photography. *IEEE Transactions on Pattern Analysis and Machine Intelligence* **44**(11), 8520–8537 (2021)
 - [134] Zhang, F., Xu, B., Li, Z., Liu, X., Lu, Q., Gao, C., Sang, N.: Towards general low-light raw noise synthesis and modeling. In: Proceedings of the IEEE/CVF International Conference on Computer Vision (ICCV), pp. 10820–10830 (2023)
 - [135] Malyugina, A., Huang, G., Ruiz, E., Leslie, B., Anantrasirichai, N.: Marine Snow Removal Using Internally Generated Pseudo Ground Truth. In: 33rd European Signal Processing Conference (EUSIPCO) (2025)
 - [136] Kousha, S., Maleky, A., Brown, M.S., Brubaker, M.A.: Modeling srgb camera noise with normalizing flows. In: Proceedings of the IEEE/CVF Conference on Computer Vision and Pattern Recognition (CVPR), pp. 17463–17471 (2022)
 - [137] Fu, Z., Guo, L., Wen, B.: srgb real noise synthesizing with neighboring correlation-aware noise model. In: Proceedings of the IEEE/CVF Conference on Computer Vision and Pattern Recognition (CVPR), pp. 1683–1691 (2023)
 - [138] Zheng, D., Zou, Y., Zhang, X., Bao, C.: Senm-vae: Semi-supervised noise modeling with hierarchical variational autoencoder. In: Proceedings of the IEEE/CVF Conference on Computer Vision and Pattern Recognition (CVPR), pp. 25889–25899 (2024)
 - [139] Monakhova, K., Richter, S.R., Waller, L., Koltun, V.: Dancing under the stars: Video denoising in starlight. In: Proceedings of the IEEE/CVF Conference on Computer Vision and Pattern Recognition (CVPR), pp. 16241–16251 (2022)
 - [140] Lin, J., Morris, C., Lin, R., Zhang, F., Bull, D., Anantrasirichai, N.: Towards a General-Purpose Zero-Shot Synthetic Low-Light Image and Video Pipeline (2025). <https://arxiv.org/abs/2504.12169>
 - [141] Anantrasirichai, N., Burn, J., Bull, D.R.: Robust texture features based on undecimated dual-tree complex wavelets and local magnitude binary patterns.

- In: 2015 IEEE International Conference on Image Processing (ICIP), pp. 3957–3961 (2015). <https://doi.org/10.1109/ICIP.2015.7351548>
- [142] Lv, F., Li, Y., Lu, F.: Attention guided low-light image enhancement with a large scale low-light simulation dataset. *International Journal of Computer Vision* **129**(7), 2175–2193 (2021)
 - [143] Yang, W., Wang, W., Huang, H., Wang, S., Liu, J.: Sparse gradient regularized deep retinex network for robust low-light image enhancement. *IEEE Transactions on Image Processing* **30**, 2072–2086 (2021) <https://doi.org/10.1109/TIP.2021.3050850>
 - [144] Triantafyllidou, D., Moran, S., McDonagh, S., Parisot, S., Slabaugh, G.: Low light video enhancement using synthetic data produced with an intermediate domain mapping. In: Vedaldi, A., Bischof, H., Brox, T., Frahm, J.-M. (eds.) *Computer Vision – ECCV 2020*, pp. 103–119. Springer, Cham (2020)
 - [145] Chen, C., Chen, Q., Do, M.N., Koltun, V.: Seeing motion in the dark. In: *Proceedings of the IEEE/CVF International Conference on Computer Vision (ICCV)* (2019)
 - [146] Zhang, Y., Ding, L., Sharma, G.: HazeRD: An outdoor scene dataset and benchmark for single image dehazing. In: *2017 IEEE International Conference on Image Processing (ICIP)*, pp. 3205–3209 (2017). <https://doi.org/10.1109/ICIP.2017.8296874>
 - [147] Wang, R., Zheng, Y., Zhang, Z., Li, C., Liu, S., Zhai, G., Liu, X.: Learning hazing to dehazing: Towards realistic haze generation for real-world image dehazing. In: *Proceedings of the Computer Vision and Pattern Recognition Conference (CVPR)*, pp. 23091–23100 (2025)
 - [148] Xu, J., Hu, X., Zhu, L., Dou, Q., Dai, J., Qiao, Y., Heng, P.-A.: Video Dehazing via a Multi-Range Temporal Alignment Network with Physical Prior. In: *2023 IEEE/CVF Conference on Computer Vision and Pattern Recognition (CVPR)*, pp. 18053–18062. IEEE. <https://doi.org/10.1109/CVPR52729.2023.01731> . <https://ieeexplore.ieee.org/document/10203534/> Accessed 2025-05-19
 - [149] Cordts, M., Omran, M., Ramos, S., Rehfeld, T., Enzweiler, M., Benenson, R., Franke, U., Roth, S., Schiele, B.: The cityscapes dataset for semantic urban scene understanding. In: *Proceedings of the IEEE Conference on Computer Vision and Pattern Recognition*, pp. 3213–3223 (2016)
 - [150] Guizilini, V., Ambrus, R., Pillai, S., Raventos, A., Gaidon, A.: 3d packing for self-supervised monocular depth estimation. In: *Proceedings of the IEEE/CVF Conference on Computer Vision and Pattern Recognition*, pp. 2485–2494 (2020)
 - [151] Wen, L., Du, D., Cai, Z., Lei, Z., Chang, M.-C., Qi, H., Lim, J., Yang, M.-H.,

- Lyu, S.: Ua-detrac: A new benchmark and protocol for multi-object detection and tracking. *Computer Vision and Image Understanding* **193**, 102907 (2020)
- [152] Zhu, P., Wen, L., Du, D., Bian, X., Fan, H., Hu, Q., Ling, H.: Detection and tracking meet drones challenge. *IEEE transactions on pattern analysis and machine intelligence* **44**(11), 7380–7399 (2021)
- [153] Pont-Tuset, J., Perazzi, F., Caelles, S., Arbeláez, P., Sorkine-Hornung, A., Van Gool, L.: The 2017 davis challenge on video object segmentation. *arXiv preprint arXiv:1704.00675* (2017)
- [154] Zhang, X., Dong, H., Pan, J., Zhu, C., Tai, Y., Wang, C., Li, J., Huang, F., Wang, F.: Learning to restore hazy video: A new real-world dataset and a new method. In: *Proceedings of the IEEE/CVF Conference on Computer Vision and Pattern Recognition (CVPR)*, pp. 9239–9248 (2021)
- [155] Li, J., Skinner, K.A., Eustice, R.M., Johnson-Roberson, M.: WaterGAN: Unsupervised Generative Network to Enable Real-time Color Correction of Monocular Underwater Images. *IEEE Robotics and Automation Letters*, 1–1 (2017) <https://doi.org/10.1109/LRA.2017.2730363> [arXiv:1702.07392](https://arxiv.org/abs/1702.07392) [cs]
- [156] Du, D., Li, E., Si, L., Xu, F., Niu, J.: End-to-end underwater video enhancement: Dataset and model. *arXiv preprint arXiv:2403.11506* (2024)
- [157] Ye, T., Chen, S., Liu, Y., Ye, Y., Chen, E., Li, Y.: Underwater light field retention: Neural rendering for underwater imaging. In: *Proceedings of the IEEE/CVF Conference on Computer Vision and Pattern Recognition (CVPR) Workshops*, pp. 488–497 (2022)
- [158] Li, C., Guo, C., Ren, W., Cong, R., Hou, J., Kwong, S., Tao, D.: An underwater image enhancement benchmark dataset and beyond. *IEEE Transactions on Image Processing* **29**, 4376–4389 (2020) <https://doi.org/10.1109/TIP.2019.2955241>
- [159] Hirsch, M., Sra, S., Schölkopf, B., Harmeling, S.: Efficient filter flow for space-variant multiframe blind deconvolution. In: *Proceedings of the IEEE Conference on Computer Vision and Pattern Recognition (CVPR)*, pp. 607–614. IEEE, ??? (2010)
- [160] Chak, W.H., Lau, C.P., Lui, L.M.: Subsampled turbulence removal network. *Mathematics and Computation in Geometry and Data* **1**(1), 1–33 (2021)
- [161] Woods, S., Kent, P., Burnett, J.G.: Lucky imaging using phase diversity image quality metric. In: *Technical Conference on Electro Magnetic Remote Sensing* (2009)
- [162] Hardie, R.C., Power, J.D., LeMaster, D.A., Bose-Pillai, D.R.D.S.: Simulation of

- anisoplanatic imaging through optical turbulence using numerical wave propagation with new validation analysis. *Optical Engineering* **56**(7), 071502 (2017) <https://doi.org/10.1117/1.OE.56.7.071502>
- [163] Mao, Z., Chimitt, N., Chan, S.H.: Accelerating atmospheric turbulence simulation via learned phase-to-space transform. In: 2021 IEEE/CVF International Conference on Computer Vision (ICCV), pp. 14739–14748 (2021). <https://doi.org/10.1109/ICCV48922.2021.01449>
 - [164] Mei, K., Patel, V.M.: Ltt-gan: Looking through turbulence by inverting gans. *IEEE Journal of Selected Topics in Signal Processing* **17**(3), 587–598 (2023) <https://doi.org/10.1109/JSTSP.2023.3238552>
 - [165] Chimitt, N., Chan, S.H.: Simulating anisoplanatic turbulence by sampling inter-modal and spatially correlated zernike coefficients. *Optical Engineering* **59**(8), 083101 (2020) <https://doi.org/10.1117/1.OE.59.8.083101>
 - [166] Anantrasirichai, N., Achim, A., Kingsbury, N.G., Bull, D.R.: Atmospheric turbulence mitigation using complex wavelet-based fusion. *IEEE Transactions on Image Processing* **22**(6), 2398–2408 (2013) <https://doi.org/10.1109/TIP.2013.2249078>
 - [167] Mao, Z., Jaiswal, A., Wang, Z., Chan, S.H.: Single frame atmospheric turbulence mitigation: A benchmark study and a new physics-inspired transformer model. In: *European Conference on Computer Vision* (2022)
 - [168] Safonov, N., Bryntsev, A., Moskalenko, A., Kulikov, D., Vatolin, D., Timofte, R., Lei, H., Gao, Q., Luo, Q., Li, Y., Song, J., Hao, S., Zheng, M., Xu, J., Wu, C., Liu, J., Chen, Y., Deng, X., Xu, M., Liang, P., Ma, J., Jin, J., Pang, Y., Luo, F., Chen, K., Zhao, S., Wu, M., Li, R., Zuo, Y., Tu, Z., Zhong, S.: Ntire 2025 challenge on ugc video enhancement: Methods and results. In: *Proceedings of the Computer Vision and Pattern Recognition Conference (CVPR) Workshops*, pp. 1503–1513 (2025)
 - [169] Zhang, Z., Xu, R., Liu, M., Yan, Z., Zuo, W.: Self-supervised image restoration with blurry and noisy pairs. In: Koyejo, S., Mohamed, S., Agarwal, A., Belgrave, D., Cho, K., Oh, A. (eds.) *Advances in Neural Information Processing Systems*, vol. 35, pp. 29179–29191. Curran Associates, Inc., ??? (2022). https://proceedings.neurips.cc/paper_files/paper/2022/file/bc12914d66b41b6bfc2d3a5decdb498b-Paper-Conference.pdf
 - [170] Poirier-Ginter, Y., Lalonde, J.-F.: Robust unsupervised stylegan image restoration. In: *Proceedings of the IEEE/CVF Conference on Computer Vision and Pattern Recognition (CVPR)*, pp. 22292–22301 (2023)
 - [171] Pinson, M.H.: Why no reference metrics for image and video quality lack accuracy and reproducibility. *IEEE Transactions on Broadcasting* **69**(1), 97–117

(2023) <https://doi.org/10.1109/TBC.2022.3191059>

- [172] Saad, M.A., Bovik, A.C.: Blind quality assessment of videos using a model of natural scene statistics and motion coherency. In: 2012 Conference Record of the Forty Sixth Asilomar Conference on Signals, Systems and Computers (ASILOMAR), pp. 332–336 (2012). <https://doi.org/10.1109/ACSSC.2012.6489018>
- [173] Lai, W.-S., Huang, J.-B., Wang, O., Shechtman, E., Yumer, E., Yang, M.-H.: Learning blind video temporal consistency. In: Proceedings of the European Conference on Computer Vision (ECCV) (2018)
- [174] Mittal, A., Soundararajan, R., Bovik, A.C.: Making a completely blind image quality analyzer. *IEEE Signal Processing Letters* **22**(3), 209–212 (2013) <https://doi.org/10.1109/LSP.2013.2295092>
- [175] Mittal, A., Moorthy, A.K., Bovik, A.C.: Blind/referenceless image spatial quality evaluator. In: 2011 Conference Record of the Forty Fifth Asilomar Conference on Signals, Systems and Computers (ASILOMAR), pp. 723–727 (2011). <https://doi.org/10.1109/ACSSC.2011.6190099>
- [176] Venkatanath, N., Praneeth, D., Chandrasekhar, B.M., Channappayya, S.S., Medasani, S.S.: Blind image quality evaluation using perception based features. In: Proceedings of the 21st National Conference on Communications (NCC). IEEE, Piscataway, NJ (2015)
- [177] Wang, J., Chan, K.C., Loy, C.C.: Exploring clip for assessing the look and feel of images. In: AAAI (2023)